

# Reducing Estimation Uncertainty Using Normalizing Flows and Stratification

Paweł Lorek<sup>1,6</sup>[0000-0003-2894-2799], Rafał Nowak<sup>2,6</sup>, Rafał Topolnicki<sup>3,6</sup>,  
Tomasz Trzciński<sup>4,6,7,8</sup>, Maciej Zięba<sup>5,6</sup>, and Aleksandra Krystecka<sup>1</sup>

<sup>1</sup> University of Wrocław, Mathematical Institute

<sup>2</sup> University of Wrocław, Institute of Computer Science

<sup>3</sup> Institute of Mathematics of the Polish Academy of Sciences (IM PAN)

<sup>4</sup> Warsaw University of Technology

<sup>5</sup> Wrocław University of Science and Technology

<sup>6</sup> Tooploox

<sup>7</sup> Jagiellonian University of Cracow

<sup>8</sup> IDEAS NCBR

**Abstract.** Estimating the expectation of a real-valued function of a random variable from sample data is a critical aspect of statistical analysis, with far-reaching implications in various applications. Current methodologies typically assume (semi-)parametric distributions such as Gaussian or mixed Gaussian, leading to significant estimation uncertainty if these assumptions do not hold. We propose a flow-based model, integrated with stratified sampling, that leverages a parametrized neural network to offer greater flexibility in modeling unknown data distributions, thereby mitigating this limitation. Our model shows a marked reduction in estimation uncertainty across multiple datasets, including high-dimensional (30 and 128) ones, outperforming crude Monte Carlo estimators and Gaussian mixture models. Reproducible code is available at <https://github.com/rnoxy/flowstrat>.

## 1 Introduction

In modern machine learning, estimating the expectation of a real-valued function  $f$  under a random variable  $\mathbf{X}$ ,

$$I = \mathbb{E} f(\mathbf{X}), \quad (1)$$

is fundamental. While  $I$  is often intractable, independent samples from  $\mathbf{X}$  are typically available. High dimensionality, multi-modality, or costly evaluations of  $f$  can render sample averages inefficient, motivating variance reduction methods. Here we consider the case where the distribution of  $\mathbf{X}$  is unknown but only  $n$  samples  $\mathbf{x}_1, \dots, \mathbf{x}_n$  are given. A naive estimator is the sample mean,  $\hat{Y}^{\text{obs}} =$

---

This is the extended version of a paper accepted for publication at ACIIDS 2026.

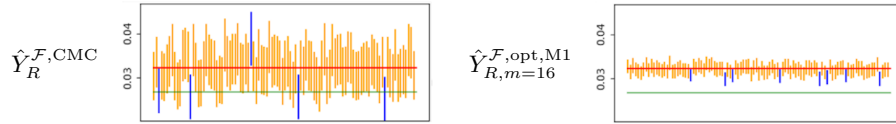


Fig. 1: Results for Example 1: 100 estimations of  $I = \mathbb{P}(X_1 > 1.2, X_2 > 1.2)$ , each (vertical line) resulted from  $R = 2^{12}$  simulations. 95% confidence intervals (vertical lines) depicted: orange lines: intervals containing true  $I$  (red line), blue lines: those not containing  $I$ . A green line – estimation of  $I$  from observations. Here  $\mathcal{F}$  means that samples  $\mathbf{x}_i$  were sampled from trained flow model, CMC stands for Crude Monte Carlo (i.e., a mean of  $f(\mathbf{x}_i)$ , no stratification) and (opt,M1) denotes specific stratification.

$\frac{1}{n} \sum_{i=1}^n f(\mathbf{x}_i)$ . Alternatively, one can estimate the distribution of  $\mathbf{X}$  and resample, often assuming a parametric family (e.g., Gaussians or mixtures), which enables stratified sampling. However, such assumptions are restrictive when the true distribution is unknown.

The *main contribution of our paper* is a model for estimating  $I = \mathbb{E} f(\mathbf{X})$  when the distribution of  $\mathbf{X}$  is unknown, relying solely on observed samples. The model uses stratified sampling (with proportional or optimal allocations) to improve accuracy, yielding more precise estimations of  $I$ . We propose two methods for stratified sampling of Gaussian distributions (cartesian and spherical) and present an effective approach for stratifying high-dimensional Gaussian distributions. To address this, we employ flow-based models [15], which map a Gaussian base distribution to complex ones via invertible neural transformations. These models provide flexible distribution estimates, from which stratified sampling improves the accuracy of  $I$ 's estimation.

The main application arises when the number of observations is *insufficient* to estimate  $I$  directly, but *sufficient* to train the flow model, enabling more accurate estimation through model-based sampling. Estimation uncertainty is further reduced via stratified sampling. For example, in estimating  $I = \mathbb{P}(X_1 > 1.2, X_2 > 1.2)$  from synthetic data, direct observation-based estimation is poor, whereas flow-based stratified sampling (with optimal allocation and 16 strata) yields more accurate results with substantially narrower 95% confidence intervals (see Fig. 1 and Table 1, row  $j_{1,2}^+$ ). For high-dimensional data, we propose two stratification methods: *cartesian*, applied to selected coordinates, and *spherical*, which stratifies only the radius and scales to high dimensions (applied in Examples 5 and 6 with  $30d$  and  $128d$ , respectively).

Normalizing flow models are known to outperform Gaussians and Gaussian mixture models (GMMs) when data come from a different distribution. This is illustrated in Example 1, where samples from this distribution are shown in Fig. 3. We compare GMM estimates with those from the trained flow model (both without stratification), as outlined in Table 5. Example 1 further shows that relatively small sample sizes suffice to train the flow model accurately, see Section 6.

## 2 Background

### 2.1 Normalizing Flows

Generative models known as normalizing flows [15,19] can be effectively trained through direct likelihood estimation by utilizing the change-of-variable formula. Continuous Normalizing Flows (CNFs) [6] propose to model transformation between data and base distributions with a dynamic system. The objective of CNFs is to solve a differential equation of the form  $\frac{d\mathbf{z}}{dt} = \mathbf{g}_\beta(\mathbf{z}(t), t)$ , where  $\mathbf{g}_\beta(\mathbf{z}(t), t)$  represents the dynamics function described by parameters  $\beta$ . The goal is to find a solution to the equation at time  $t_1$ ,  $\mathbf{y} := \mathbf{z}(t_1)$ , given an initial state  $\mathbf{z} := \mathbf{z}(t_0)$  with a known prior. The transformation function  $\mathbf{h}_\beta$  and the log-density of  $\mathbf{x}$  are as follows:

$$\begin{aligned} \mathbf{x} &= \mathbf{h}_\beta(\mathbf{z}) = \mathbf{z} + \int_{t_0}^{t_1} \mathbf{g}_\beta(\mathbf{z}(t), t) dt, \\ \log p_\beta(\mathbf{x}) &= \log \mathcal{N}(\mathbf{z}; \mathbf{0}, \mathbf{I}) - \int_{t_0}^{t_1} \frac{d\mathbf{h}_\beta(\mathbf{z}(t), t)}{d\mathbf{z}(t)} dt. \end{aligned} \quad (2)$$

The decision to use CNFs is driven by successful applications in models such as NGGP [17], PointFlow [22], and StyleFlow [1], which are characterized by similar dimensionalities.

### 2.2 Monte Carlo estimation

Here, we assume we aim to estimate the expectation of a random variable  $Y \in \mathbb{R}$ , namely  $I = \mathbb{E}Y$ , given that we can sample  $Y$  and know that  $\mathbb{E}Y^2 < \infty$ . (Later we consider  $Y = f(\mathbf{X})$ ,  $f: \mathbb{R}^d \rightarrow \mathbb{R}$ ). Suppose we have  $R \geq 1$  samples  $Y_1, \dots, Y_R$ , and  $\hat{Y}_R$  is an unbiased estimator of  $I$  (i.e.,  $\mathbb{E}\hat{Y}_R = I$ ) based on these samples. Then, the central limit theorem (CLT) states that for any  $\alpha \in (0, 1)$ , we have (in our applications  $R$  is large, making the CLT approximation accurate)

$$\mathbb{P} \left( I \in \left[ \hat{Y}_R \pm z_{1-\alpha/2} \sqrt{\widehat{\text{Var}}(\hat{Y}_R)} \right] \right) \approx 1 - \alpha. \quad (3)$$

Thus, the smaller the estimator's variance, the narrower the above confidence interval.

*Crude Monte Carlo estimator.* The simplest estimator, usually called *Crude Monte Carlo estimator*, is a sample mean of iid  $Y_1, \dots, Y_R$ , namely  $\hat{Y}_R^{\text{CMC}} = \sum_{j=1}^R Y_j / R$ . In such a case, we have  $\text{Var}(\hat{Y}_R^{\text{CMC}}) = \text{Var}Y / R$ . In practice we often do not know  $\text{Var}Y$ , we may however replace it with a sample variance  $\hat{S}_R^2 = \sum_{j=1}^R (Y_j - \hat{Y}_R^{\text{CMC}})^2 / (R-1)$ , since a version of CLT states that  $\sum_{j=1}^R (Y_j - I) / (\hat{S}_R \sqrt{R})$  converges to a standard normal  $\mathcal{N}(0, 1)$  as  $R \rightarrow \infty$ . In other words, we have the confidence interval given by Eq. (3) with  $\text{Var}(\hat{Y}_R)$  replaced with  $\hat{S}_R^2 / R$ .

### 2.3 Stratified sampling

Fix  $m \geq 1$  (number of strata) and let  $A^1, \dots, A^m$  be disjoint sets such that  $\mathbb{P}(Y \in \cup_{j=1}^m A^j) = 1$ . This split defines *strata*  $S^j = \{\omega : Y(\omega) \in A^j\}$ . Slightly abusing the notation, we will call  $A^j$  also a stratum. We assume that  $m$  and strata  $A^j, j = 1, \dots, m$  are fixed. Let  $p_j = \mathbb{P}(Y \in A^j)$  be the probability of  $j$ -th stratum and let  $I^j = \mathbb{E}[Y|Y \in A^j]$  be the expectation of  $Y$  on  $j$ -th stratum. The law of total expectation yields

$$I = \mathbb{E}Y = p_1 I^1 + \dots + p_m I^m. \quad (4)$$

The idea of stratified sampling can be thus explained as follows. Split the total budget of simulations (*general split*)  $R = R_1 + \dots + R_m$ , then estimate  $I^j$  using  $R_j$  simulations and finally estimate  $I$  computing the weighted average (4). Note that to apply the procedure, we need to be able to sample  $Y$  from  $j$ -th stratum, i.e.,  $Y^j \stackrel{\mathcal{D}}{=} (Y|Y \in A^j)$  (equality in distribution). Let  $Y_1^j, \dots, Y_{R_j}^j$  be iid replications of  $Y^j$ . We estimate  $I^j$  via  $\hat{Y}_{R_j}^j = \frac{1}{R_j} \sum_{i=1}^{R_j} Y_i^j$  (which is a CMC estimator of  $I^j$ ). Finally, denoting,  $\sigma_j^2 = \text{Var} Y^j$ , the *stratified estimator* and its variance are:

$$\hat{Y}_R^{\text{str}} = p_1 \hat{Y}_{R_1}^1 + \dots + p_m \hat{Y}_{R_m}^m, \text{Var}(\hat{Y}_R^{\text{str}}) = \sum_{j=1}^m \frac{p_j^2}{R_j} \sigma_j^2.$$

Again, in practice, we do not know the variances  $\sigma_j^2$ , we estimate them via sample variances  $\hat{s}_j^2$  and we estimate the variance of  $\hat{Y}_R^{\text{str}}$  via  $\widehat{\text{Var}}(\hat{Y}_R^{\text{str}}) = \sum_{j=1}^m \frac{p_j^2}{R_j} \hat{s}_j^2$ .

*Proportional allocation.* We split  $R$  proportionally to probabilities of strata, i.e.,  $R_j = R p_j$ . Denote the corresponding estimator as  $\hat{Y}_R^{\text{pa}}$ . Then we have  $\text{Var}(\hat{Y}_R^{\text{pa}}) = \frac{1}{R} \sum_{j=1}^m p_j \sigma_j^2$  and  $\widehat{\text{Var}}(\hat{Y}_R^{\text{pa}}) = \frac{1}{R} \sum_{j=1}^m p_j \hat{s}_j^2$ . A variance of CMC estimator may be decomposed as  $\text{Var}(\hat{Y}_R^{\text{CMC}}) = \text{Var}(\hat{Y}_R^{\text{pa}}) + \sum_{j=1}^m p_j (I^j - I)^2$ , thus  $\text{Var}(\hat{Y}_R^{\text{pa}}) \leq \text{Var}(\hat{Y}_R^{\text{CMC}})$ .

*Optimal allocation.* It turns out that the split:  $R_j = \frac{p_j \sigma_j}{\sum_{i=1}^m p_i \sigma_i} R, \quad j = 1, \dots, m$ , is best possible, in the sense that  $\text{Var}(\hat{Y}_R^{\text{opt}}) \leq \text{Var}(\hat{Y}_R^{\text{str}})$ , where  $\hat{Y}_R^{\text{opt}}$  is the stratified estimator with above split and  $\hat{Y}_R^{\text{str}}$  is a general stratified estimator. The proof of this fact (formally in Theorem A1 in appendix) and the decomposition of CMC variance may be found e.g., in [10] (Theorem 3.3), in Appendix A.1 we provide different proofs.

## 3 Methodology of our method

### 3.1 Stratifying multivariate Gaussian

The two methods described below are presented for equally probable strata (i.e.,  $p_i = 1/m$ ), as we will need only this form (it generalizes easily).

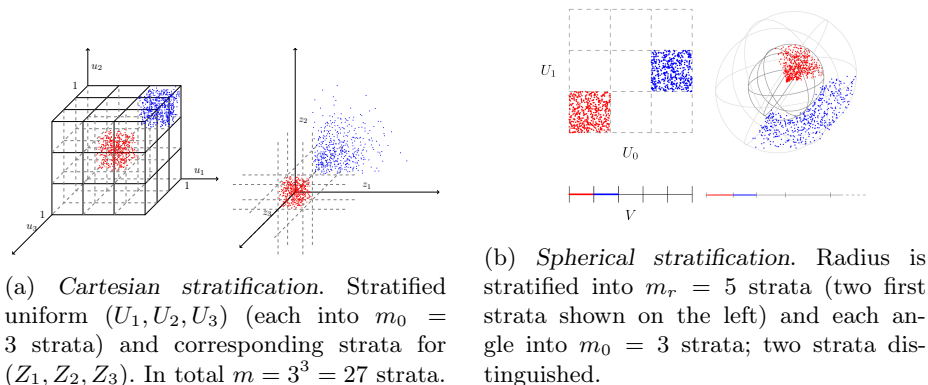


Fig. 2: Comparison of Cartesian and Spherical stratifications.

**Method M1: Cartesian stratification** Let us start with a univariate standard normal  $Z \sim \mathcal{N}(0, 1)$ , denoting its distribution function by  $\Phi$ . To perform stratified sampling with  $m_0$  strata, we split  $\mathbb{R}$  into  $m_0$  intervals:

$$A^1 = (a_0, a_1], \dots, A^{m_0} = (a_{m_0-1}, a_{m_0}], \quad (5)$$

where  $a_0 = -\infty$ ,  $a_{m_0} = +\infty$ , and  $a_j$  are chosen so that  $\mathbb{P}(Z \in (a_{j-1}, a_j]) = p_j$ , achieved by setting  $a_1 = \Phi^{-1}(p_1)$ ,  $a_2 = \Phi^{-1}(p_1 + p_2), \dots$  (inverses  $\Phi^{-1}(\cdot)$  are evaluated numerically). To sample  $Z^j$  from  $A^j$ , we take  $U \sim \mathcal{U}(0, 1)$  and set  $Y^j = \Phi^{-1}(V^j)$ , where  $V^j = a_{j-1} + (a_j - a_{j-1})U$ . Now, let  $(Z_1, \dots, Z_d)$  be a standard normal  $d$ -dimensional random variable. We split each  $Z_i$  into  $m_0$  strata as above, obtaining  $m = m_0^d$  strata. If  $p_j = 1/m_0$  for each  $Z_i$ , we obtain  $m_0^d$  equally probable strata.

Consider the example: to sample a 3D standard normal point  $(Z_1, Z_2, Z_3)$ , we can sample  $(U_1, U_2, U_3)$  uniformly from the hypercube  $[0, 1]^3$  and compute  $Z_i = \Phi^{-1}(U_i)$ ,  $i = 1, 2, 3$ . Now, if we sample  $(U_1, U_2, U_3)$  only from one of nine sub-hypercubes (of equal volume), the resulting  $(Z_1, Z_2, Z_3)$  will be a normally distributed 3D point sampled from the corresponding stratum. In Fig. 2a, two such strata are illustrated.

**Method M2: Spherical stratification** **Stratification with respect to radius.** The random variable  $D^2 = Z_1^2 + \dots + Z_d^2$  follows a  $\chi_d^2$  distribution (chi-squared with  $d$  degrees of freedom) with cdf  $F_{\chi_d^2}$ . Thus, if we sample  $d$  iid standard normal  $\mathcal{N}(0, 1)$  variables, collect them as  $\mathbf{Z} = (Z_1, \dots, Z_d)$ , normalize them as  $\mathbf{Z}' = \left( \frac{Z_1}{\|\mathbf{Z}\|}, \dots, \frac{Z_d}{\|\mathbf{Z}\|} \right)$ , and then set  $\mathbf{Z}'' = (DZ'_1, DZ'_2, \dots, DZ'_d)$ , where  $D^2$  is sampled from a  $\chi_d^2$  distribution, then  $\mathbf{Z}''$  has the same distribution as  $\mathbf{Z}$ . This leads to the following stratification. Fix the number of strata  $m_r$ , sample standard normal variables  $Z_1, \dots, Z_d$ , and normalize them (obtaining  $Z'_1, \dots, Z'_d$ ). Now, stratify only the radius  $D$  by sampling it from the  $j$ -th stratum, which is

done by sampling  $U \sim \mathcal{U}(0, 1)$  and setting  $(D^j)^2 = F_{\chi_d^2}^{-1} \left( \frac{j}{m_r} + \frac{1}{m_r} U \right)$ , to finally obtain  $\mathbf{Z}^j = (D^j Z'_1, \dots, D^j Z'_d)$ .

**Stratification w.r.t. angles.** Multivariate standard normal  $\mathbf{Z} = (Z_1, \dots, Z_d)$  normalized (i.e.,  $\mathbf{Z}' = \mathbf{Z}/\|\mathbf{Z}\|$ ) has a uniform distribution on the hypersphere

$$S_{d-1} = \left\{ \mathbf{x} = (x_1, \dots, x_d) : \sum_{j=1}^d x_j^2 = 1 \right\}.$$

A point  $\mathbf{x} \in S_{d-1}$  can be represented in spherical coordinates as

$$\begin{aligned} x_1 &= \cos \phi_1, & x_2 &= \sin \phi_1 \cos \phi_2, & \dots, \\ x_d &= \sin \phi_1 \cdots \sin \phi_{d-3} \sin \phi_{d-2} \sin \theta, \end{aligned} \quad (6)$$

where  $\phi_1, \dots, \phi_{d-2} \in [0, \pi)$  and  $\theta \in [0, 2\pi)$ . The density of the uniform distribution on  $S_{d-1}$  (in these coordinates) factorizes as

$$g(\theta, \phi_1, \dots, \phi_{d-2}) \propto \sin^{d-2} \phi_1 \sin^{d-3} \phi_2 \cdots \sin \phi_{d-2},$$

which can be written as a product of one-dimensional densities

$$g(\theta, \phi_1, \dots, \phi_{d-2}) = h_0(\theta) h_1(\phi_1) \cdots h_{d-2}(\phi_{d-2}),$$

where  $h_0$  is the density of the uniform distribution on  $(0, 2\pi)$  and

$$h_k(\phi) = \frac{1}{c_k} \sin^k(\phi), \quad \phi \in (0, \pi), \quad k = 1, \dots, d-2,$$

with normalization constants  $c_k = \int_0^\pi \sin^k(x) dx$ . Consequently, sampling uniformly from  $S_{d-1}$  reduces to independent sampling of  $\theta \sim h_0$  and  $\phi_k \sim h_k$  for  $k = 1, \dots, d-2$ .

To obtain stratified sampling on the hypersphere, we stratify each angular coordinate. For  $\theta$  we split  $(0, 2\pi)$  into  $m_0$  equal-length intervals. For each  $\phi_k$  we construct  $m_0$  strata  $(a_{k,j-1}, a_{k,j}]$  such that

$$\int_{a_{k,j-1}}^{a_{k,j}} h_k(\phi) d\phi = \frac{1}{m_0}, \quad j = 1, \dots, m_0,$$

which is done numerically. Sampling from a given stratum then consists in drawing  $\theta$  and  $\phi_k$  from the corresponding one-dimensional strata and mapping  $(\theta, \phi_1, \dots, \phi_{d-2})$  back to a point on  $S_{d-1}$  via (A6). Combining this with stratification of the radius (as in the previous paragraph) yields  $m = m_r m_0^{d-2}$  equally probable strata for the Gaussian base distribution.

The one-dimensional densities  $h_k(\phi) \propto \sin^k(\phi)$  do not admit closed-form inverse distribution functions for general  $k$ . In practice, we therefore generate samples from  $h_k$  using a simple acceptance–rejection scheme with a uniform proposal on  $(0, \pi)$  and extend it to stratified sampling by restricting the proposal to a chosen

subinterval. The expected number of accept–reject iterations remains moderate even for large  $k$ , which makes the method practical in our settings. Full derivations, the explicit form of the acceptance–rejection sampler and construction of the boundaries  $a_{k,j}$  are provided in Appendix A.2.

**Full stratification.** We simply independently stratify radius  $D$  (using  $m_r$  strata) and angles  $\theta, \phi_1, \dots, \phi_{d-2}$  (using  $m_0$  strata for each angle) as described above, thus finally we have  $m = m_r m_0^{d-2}$  equally probable strata. The case  $d = 3$  with  $m_r = 5$  and  $m_0 = 3$  is depicted in Fig. 2b.

### 3.2 Optimal allocation in practice

First, we run  $R'$  pilot simulations (usually much smaller than target  $R$  simulations) with proportional allocation just to estimate variances  $\hat{s}_j'^2$  in each strata. They serve to compute the final optimal split  $R_j = \frac{p_j \hat{s}_j'^2}{\sum_{k=1}^m p_k \hat{s}_k'^2} R$ . Then we perform  $R_j$  simulations  $Y_1^j, \dots, Y_{R_j}^j$  in each stratum  $j = 1, \dots, m$ , estimate  $I^j$  via  $\hat{Y}_{R_j}^j$  and compute the final estimator  $\hat{Y}_R^{\text{opt}} = p_1 \hat{Y}_{R_1}^1 + \dots + p_m \hat{Y}_{R_m}^m$ . Afterwards we recompute variances  $\hat{s}_j^2$  within each stratum and estimate  $\text{Var} \hat{Y}_R^{\text{opt}}$  via  $\widehat{\text{Var}}(Y_R^{\text{opt}}) = \left( \sum_{j=1}^m p_j \hat{s}_j \right)^2$ .

### 3.3 High-dimensional stratification

When  $d$  is large, using Method M1 (cartesian) or Method M2 (spherical) with  $m_0 > 1$  strata in every dimension or angle leads to an exponential number of strata ( $m_0^d$  or  $m_r m_0^{d-2}$ ), which is prohibitive in our 30- and 128-dimensional examples. We therefore use two approximations.

*Method Mrad.* This method is a special case of spherical stratification. We stratify only the radius  $D$  into  $m_r$  equally probable shells and do not stratify the angles ( $m_0 = 1$ ). In other words,  $\mathbb{R}^d$  is split into  $m = m_r$  radial strata  $A^1, \dots, A^m$ , and we sample  $\mathbf{Z}^j \stackrel{\mathcal{D}}{=} (\mathbf{Z} \mid \mathbf{Z} \in A^j)$  by first sampling a direction on the sphere and then sampling the radius from the  $j$ -th  $\chi_d^2$ -stratum as in Section 3.1. The resulting estimators are denoted  $\hat{Y}_{R,m}^{\mathcal{F},\text{prop},\text{Mrad}}$  and  $\hat{Y}_{R,m}^{\mathcal{F},\text{opt},\text{Mrad}}$  for proportional and optimal allocation, respectively.

*Methods MHigh3 and MRand3.* Here we stratify only  $\eta = 3$  selected coordinates into  $m_0$  strata each, which yields  $m = m_0^3$  equally probable strata. For a given triple  $(i, j, k)$  we use the one-dimensional normal stratification from Section 3.1 on coordinates  $Z_i, Z_j, Z_k$  and keep the remaining coordinates unstratified. Sampling from a given stratum is then straightforward: we sample  $Z_t \sim \mathcal{N}(0, 1)$  for  $t \notin \{i, j, k\}$  and sample  $Z_i, Z_j, Z_k$  from the corresponding one-dimensional intervals.

In Method MRand3 the indices  $i, j, k$  are chosen uniformly at random from  $\{1, \dots, d\}$  (independently in each repetition). In Method MHigh3 the choice depends on the target function  $f$  to be estimated. We first run  $R_0 < R$  pilot

simulations and, for each coordinate  $b$ , construct a stratified estimator that splits only  $Z_b$  into  $m_0$  strata. We then compute the empirical standard deviations of these  $d$  estimators and select the three coordinates with the largest variances as  $i, j, k$ . The corresponding estimator is denoted  $\hat{Y}_{R,m=m_0^3}^{\mathcal{F},\text{prop},\text{MHigh3}}$ . Further implementation details are provided in Appendix A.3.

### 3.4 Stratified flow-based estimation

Given  $n$  observations  $\mathbf{x}_1, \dots, \mathbf{x}_n$  from  $\mathbb{R}^d$ , we first approximate their distribution  $p(\mathbf{x})$  by  $p_\beta(\mathbf{x})$  by training a flow model  $\mathcal{F}_\beta$  to minimize the negative log-likelihood  $\mathcal{L} = -\sum_{k=1}^n \log p_\beta(\mathbf{x}_k)$ , with respect to the parameters  $\beta$ , where  $\log p_\beta(\cdot)$  is given by Eq. (2). This loss is optimized using a standard, gradient-based training procedure, as described in [6]. Once the flow model is trained, we can sample any number of points from  $p_\beta(\mathbf{x})$ , which approximates the distribution  $p(\mathbf{x})$  of the random variable  $\mathbf{X}$ . Direct stratification in the data space is challenging, so we propose stratifying in the latent space of the flow model, with the Gaussian base distribution  $p(\mathbf{z}) = \mathcal{N}(\mathbf{z}; \mathbf{0}, \mathbf{I})$ . We then apply either Method 1 (cartesian) or Method 2 (spherical) to split the Gaussian latent space and generate the desired number of points (proportional or optimal) in each region. The points generated in each region are then transformed to the data space using the transformation  $\mathbf{h}_\beta(\mathbf{z})$  defined by Eq. (2). Afterward, we apply  $f$  to the generated points and estimate  $I = \mathbb{E} f(\mathbf{X})$ . Note that if we need to estimate multiple quantities  $I_k = \mathbb{E} f_k(\mathbf{X})$ ,  $k = 1, \dots, M$ , the flow model requires only a single training.

## 4 Experimental results

For a random variable  $\mathbf{X}$ , we want to estimate  $I = \mathbb{E} f(\mathbf{X})$  based on observations  $\mathbf{x}_1, \dots, \mathbf{x}_n$ . An exact value of  $I$  is known for all synthetic examples (in Example 3, an "exact" value is computed by sampling a large number of points). Recall,  $\hat{Y}_n^{\text{obs}} = \sum_{i=1}^n f(\mathbf{x}_i)/n$  estimates  $I$  from observations. After training a flow model  $\mathcal{F}_\beta$ , we construct the following estimators of  $I$ : i)  $\hat{Y}_R^{\mathcal{F},\text{CMC}} = \frac{1}{R} \sum_{i=1}^R f(\mathbf{x}_i^{\mathcal{F}})$  – we simply sample  $R$  points  $\mathbf{x}_1^{\mathcal{F}}, \dots, \mathbf{x}_R^{\mathcal{F}}$  from  $\mathcal{F}_\beta$  (via independent sampling of base distribution rvs) and compute means of  $f(\mathbf{x}_i^{\mathcal{F}})$ ; ii)  $\hat{Y}_{R,m=k}^{\mathcal{F},\text{prop},\text{M}}$  – we sample  $R$  points using stratification with proportional sampling and stratification method  $\text{M} \in \{\text{M1}, \text{M2}, \text{Mrad}, \text{MHigh3}, \text{MRand3}\}$  and  $k$  strata; iii)  $\hat{Y}_{R,m=k}^{\mathcal{F},\text{opt}}$  – similarly, we use stratification with optimal allocation (where we also used  $R'$  pilot simulations to estimate stratum variances). For optimal allocation, unless stated otherwise, we use  $R' = R/8$  pilot simulations to estimate standard deviations.

We compute:  $\mathbf{E}$  – the estimator value, an approximation of  $I$ ;  $\mathbf{SD}$  – the standard deviation of the estimator; and  $\mathbf{AC} = -\log_{10} |(I - \mathbf{E})/I|$ , the estimator’s accuracy (roughly speaking, the number of correct digits in  $\mathbf{E}$ ). In tables, we report  $I$ ,  $\mathbf{E}$ ,  $\mathbf{SD}$ ,  $\mathbf{AC}$ , or (for readability)  $I^* = 100I$ ,  $\mathbf{SD}^* = 100\mathbf{SD}$ , and  $\mathbf{E}^* = 100\mathbf{E}$ .

All metric values are computed as **means of 10 simulations**. Note that the average of 10  $\mathbf{AC}$  values is **not** equal to  $\mathbf{AC}$  computed from the average of 10  $\mathbf{E}$  values. Metrics are presented in tables rounded to three or four digits, though

they are computed with higher precision. Data in tables allow for constructing a confidence interval at level  $\alpha$ , namely  $\mathbb{P}(\hat{Y} - z_{1-\alpha/2}\text{SD} \leq I \leq \hat{Y} + z_{1-\alpha/2}\text{SD}) \approx 1 - \alpha$ , Fig. 1 presents confidence intervals for Example 1.

In examples with known  $I$ , in tables, the best accuracy in each row is **bolded**, second best is underlined, unless otherwise stated in a caption. In examples with unknown  $I$ , neither  $I$  nor **AC** are reported, then the best (smallest) **SD** is **bolded**, and the second best (second smallest) **SD** is underlined. We consider different functions  $f$  across examples, with the following functions often used:

$$j_t^+(\mathbf{x}) = \mathbf{1}(\forall i : x_i > t), \quad j_t^-(\mathbf{x}) = \mathbf{1}(\forall i : x_i \leq t), \quad (7)$$

which estimate probabilities  $\mathbb{P}(X_i > t, i = 1, \dots, d)$  and  $\mathbb{P}(X_i \leq t, i = 1, \dots, d)$ . We demonstrate examples with different parameters  $n, m, R$  and functions  $f$  to show the robustness of the method, yielding superior results over observation-based estimations.

**Example 1.** Random vector  $\mathbf{X} = (X_1, X_2)^T$  has a density  $g(x_1, x_2) = x_1 \exp(-x_1(x_2 + 1))$  for  $x_1, x_2 \geq 0$ . The exponential  $g_{X_1}(x_1) = e^{-x_1}$  and Pareto  $g_{X_2}(x_2) = (x_2 + 1)^{-2}$  distributions are marginal distributions of  $g$  (in Appendix A.4.2 we describe how to sample from  $g$ ). We will estimate  $I = \mathbb{P}(X_1 > t, X_2 > t)$  for  $t \in \{0.9, 1.0, 1.2\}$  (i.e.,  $\mathbb{E} j_t^+(\mathbf{X})$ ) and expectations of:

Table 1: (Example 1) Results for **cartesian** method.

$f$	$I^*$	$\hat{Y}_{1000}^{\text{obs}}$		$R$	$\hat{Y}_R^{\mathcal{F}, \text{CMC}}$		$\hat{Y}_{R, m=4 \times 4}^{\mathcal{F}, \text{opt}, \text{M1}}$	
		<b>E*</b>	<b>AC</b>		<b>E*</b>	<b>AC</b>	<b>E*</b>	<b>AC</b>
$j_{1.2}^+$	3.24	2.70	.776	$2^{12}$	3.14	<u>1.25</u>	3.24	<b>1.82</b>
				$2^{15}$	3.23	<u>1.81</u>	3.22	<b>2.22</b>
$j_{2.0}^+$	.080	.000	.000	$2^{12}$	.08	<u>.613</u>	.09	<b>1.06</b>
				$2^{15}$	.10	<u>.668</u>	.10	<b>.693</b>
$h_1$	12.3	10.1	.755	$2^{12}$	11.6	<u>1.10</u>	12.0	<b>1.63</b>
				$2^{15}$	12.2	<u>1.54</u>	12.1	<b>1.83</b>
$h_2$	3.18	2.75	.868	$2^{12}$	3.03	<u>1.35</u>	3.07	<b>1.50</b>
				$2^{15}$	3.07	<b>1.50</b>	3.07	<u>1.47</u>

$$h_1(\mathbf{x}) = (\log |x_1 x_2|)^{-1} j_1^+(\mathbf{x}), \quad h_2(\mathbf{x}) = \sin(x_1 x_2) j_1^+(\mathbf{x}), \quad h_3(\mathbf{x}) = (x_1 x_2)^{-1} j_1^+(\mathbf{x}). \quad (8)$$

We trained the model on 1000 observations, then estimated  $I$  using  $R \in \{2^{12}, 2^{15}\}$  replications.

The results for cartesian stratification are gathered in Table 1 (only **E** and **AC** and one model reported, more results are provided in Appendix in Table A1).

In Fig. 3, two stratification methods are illustrated.

In Fig. 1, estimations and corresponding 95% confidence intervals from 100 simulations for  $\hat{Y}_R^{\mathcal{F}, \text{CMC}}$  and  $\hat{Y}_{R, m=16}^{\mathcal{F}, \text{opt}, \text{M1}}$ , both with  $R = 2^{12}$ , are shown. As expected from theory, the probability that a

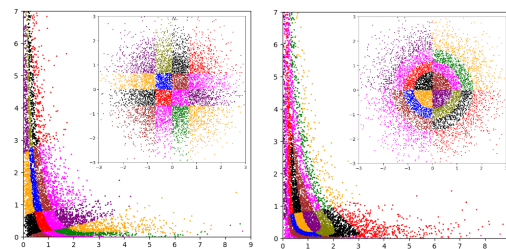


Fig. 3: Example 1:  $R = 2^{13}$  points and  $m = 16$  strata. Cartesian (left column) and spherical (right column). Smaller plots: 2D iid standard normal; larger plots: points mapped through  $\mathcal{F}$ , colors denote corresponding strata.

confidence interval includes

the true value of  $I$  is 95%: 5% of CMC estimator intervals and 8% of stratified estimator intervals did not contain  $I$  (the number of intervals not containing  $I$  follows a binomial distribution with parameters 100 and 0.05; observing  $\{3, \dots, 8\}$  such intervals is quite likely with probability 0.81). Confidence intervals for other estimators (as in Table 1 and Table A1), for spherical stratification (yielding similar conclusions), and a comparison of methods M1 and M2 are provided in Appendix A.4.2.

*Common conclusions for Example 1 and Example A1 (from the Appendix).* In both cases  $n = 1000$  points were not enough to estimate  $I$  correctly from data, but they sufficed to train the flow model correctly, which in turn resulted in better estimations of  $I$  (in Example 1 even  $n = 500$  points suffices, see Appendix A.4.1 for details). In both examples accuracy from flow models were better than from data, best accuracy was always obtained for some stratified estimator. In all cases the variance of CMC estimator was smaller than variance of  $\hat{Y}_{1000}^{\text{obs}}$  and in majority of cases, the variance any stratified estimator was better than the variance of CMC. Summarizing, not only the point estimates (AC) are better using M1 or M2 methods, but also uncertainty in such cases is smaller.

**Example 2.** Let  $\mathbf{X} = (X_1, \dots, X_d)^T$  be a  $d$  dimensional multivariate Student's  $t$ -distribution with  $\nu = 5$  degrees of freedom, mean  $\boldsymbol{\mu} = (0, \dots, 0)^T$  and with matrix  $\boldsymbol{\Sigma}(i, i) = 1$  and  $\boldsymbol{\Sigma}(i, j) = 0.2$  for  $i, j \in \{1, \dots, d\}, j \neq i$ , i.e., with density  $\frac{\Gamma((\nu+d)/2)}{\Gamma(\nu/2)\nu^{d/2}\pi^{d/2}|\boldsymbol{\Sigma}|} (1 + \frac{1}{\nu}\mathbf{x}^T\boldsymbol{\Sigma}^{-1}\mathbf{x})^{-(\nu+d)/2}$ . For  $d = 3$  and  $d = 4$  we aim at estimating  $\mathbf{E} h_j(\mathbf{X}), j \in \{1, 2, 3\}$ , where  $h_j(\mathbf{x})$  are defined in (8) and adopted to  $d = 3$  and  $d = 4$ . In this example we performed simulations for larger  $n = 20k$  and  $R \in \{50k, 100k, 500k\}$ , we considered up to  $m = 1296$  strata.

Table 2: (Example 2,  $d = 4$ ) Numerical results for **cartesian** (method M1) and **spherical** (method M2) stratification. The true value is  $I^*$  is  $-0.033$  for  $h_1$ ,  $.0993$  for  $h_2$  and  $.400$  for  $h_3$ .

$t$	$\hat{Y}_{20k}^{\text{obs}}$			$R$	$\hat{Y}_R^{\mathcal{F}, \text{CMC}}$			$\hat{Y}_{R, m=6 \times 6 \times 6}^{\mathcal{F}, \text{prop}, \text{M1}}$			$\hat{Y}_{R, m=6 \times 6 \times 6}^{\mathcal{F}, \text{opt}, \text{M1}}$			$\hat{Y}_{R, m=10 \times 5 \times 5}^{\mathcal{F}, \text{prop}, \text{M2}}$			$\hat{Y}_{R, m=10 \times 5 \times 5}^{\mathcal{F}, \text{opt}, \text{M2}}$		
	E*	SD*	AC		E*	SD*	AC	E*	SD*	AC	E*	SD*	AC	E*	SD*	AC	E*	SD*	AC
$h_1$	.015	.485		50k	-.055	.299	<u>.20</u>	-.003	.313	-.13	-.047	.043	.09	-.028	.296	<b>.36</b>	-.072	.048	-.07
				100k	-.023	.214	<b>.62</b>	-.026	.216	.38	-.020	.034	.28	-.012	.211	.12	-.037	.035	<u>.47</u>
				500k	-.028	.097	.44	-.023	.096	.571	-.041	.020	.72	-.035	.095	<b>1.1</b>	-.029	.016	<u>.90</u>
$h_2$	.103	.105	.986	50k	.098	.062	1.3	.098	.050	<u>1.3</u>	.109	.007	.82	.091	.052	<b>1.5</b>	.084	.006	.99
				100k	.096	.044	1.5	.094	.035	<b>1.8</b>	.092	.006	1.6	.093	.036	<u>1.6</u>	.084	.005	1.1
				500k	.095	.019	1.7	.096	.016	<u>1.8</u>	.095	.003	1.8	.092	.016	<b>2.3</b>	.093	.003	1.7
$h_3$	.423	.351	1.24	50k	.416	.215	1.5	.408	.161	<u>1.5</u>	.427	.021	1.4	.395	.173	<b>1.6</b>	.402	.021	1.2
				100k	.410	.151	<u>1.7</u>	.414	.111	1.5	.393	.017	1.2	.394	.126	<b>1.8</b>	.392	.017	1.4
				500k	.412	.068	1.7	.411	.050	1.6	.400	.009	<b>3.1</b>	.401	.054	<u>2.1</u>	.432	.009	1.4

Results for  $d = 4$  are presented in Table 2 (results for  $d = 3$  are provided in Appendix A.4.2). As expected the variance of the stratified estimator with optimal allocation is lower than the variance of the proportionally stratified counterpart, which in turn is lower than the variance of CMC estimator. In most cases, the accuracy of the stratified estimator is higher than the one obtained in CMC method. In majority of considered cases the flow-based estimate yielded

higher accuracy than the estimate obtained from train data. Similar conclusions can be drawn for estimations of  $\mathbf{E} j_t^+(\mathbf{X})$  (experiments results not shown).

**Example 4 (Real-world example).** For a real-world scenario, we considered 2-dimensional data from the AmeriGEOSS [20] dataset containing wind measurements in Papua New Guinea.

We chose the mean and standard deviation of air pressure (after applying a standard difference transform) collected between 02/15/18 and 02/28/19. We trained the model on the first 3000 observations, with training conducted over 2000 epochs (all other parameters of the flow model are as in Example 1). We estimated the following functions:

Table 3: (Example 4) Numerical results for **spherical** (method M2) stratification.

$F$	$\hat{Y}_{3000}^{\text{obs}}$		$R$	$\hat{Y}_R^{\mathcal{F},\text{CMC}}$		$\hat{Y}_{R,2 \times 2}^{\mathcal{F},\text{opt}}$		$\hat{Y}_{R,4 \times 4}^{\mathcal{F},\text{opt}}$	
	E	SD*		E	SD*	E	SD*	E	SD*
$g_1$	.192	.719	$2^{12}$	.194	.618	.191	<u>.371</u>	.193	<b>.175</b>
			$2^{15}$	.194	.218	.193	<u>.131</u>	.193	<b>.064</b>
$g_2$	.001	.087	$2^{12}$	.001	.075	.001	<u>.035</u>	.001	<b>.034</b>
			$2^{15}$	.001	.026	.001	<u>.012</u>	.001	<b>.010</b>
$g_3$	.004	.009	$2^{12}$	.004	.008	.004	<u>.005</u>	.004	<b>.004</b>
			$2^{15}$	.004	.003	.004	<u>.001</u>	.004	<b>.001</b>

$$g_1(x_1, x_2) = \mathbf{1}(\max(x_1, x_2) > 0.01), \quad g_2(x_1, x_2) = \frac{x_2}{(1 + x_1^2)}, \quad g_3(x_1, x_2) = |x_1 x_2|.$$

The results for spherical stratification are provided in Table 3. In Appendix A.4.5 we present results for additional functions, as well as for cartesian stratification, and show the training data and samples from the flow model. Note that we do not know the exact values of  $I_i = \mathbf{E} g_i(\mathbf{X})$ , so we focus on methods with the smallest SD. In all cases, the stratified estimator with optimal allocation and 16 strata gave the best results. In many cases, the estimated values are very similar – e.g., for  $g_3$ , all estimators produced a value of 0.0046 (differing only in further decimal places); however, using spherical stratification with 16 strata and optimal allocation yielded the smallest SD, indicating that with high probability the true value of  $I$  lies in a narrow interval  $[0.0046 \pm z_{1-\alpha/2}\text{SD}]$  (cf. Fig. 1).

The next two examples address a problem of stratification in higher dimensions.

**Example 5 (30D).** Synthetic 30-dimensional example: most coordinates are independent with different distributions and parameters, while some (non-consecutive) are multivariate non-standard normal. A precise description, including a pair-plot, is provided in Appendix A.4.6. The flow model was trained on only  $n = 500$  observations. For the **Mrad** method, we stratify the radius into  $m \in \{3, 7\}$  strata, while for **MHigh3** and **MRand3**, we stratify three selected dimensions into  $m_0 = 3$  strata (resulting in  $3^3 = 27$  strata). Detailed numerical results for estimating  $j_t^+$  for  $t \in \{-1.0, -0.8, -0.6\}$  with  $R \in \{2^{12}, 2^{13}\}$ , namely estimators  $\hat{Y}_{R,m=3}^{\mathcal{F},\text{prop},\text{Mrad}}$ ,  $\hat{Y}_{R,m=3}^{\mathcal{F},\text{opt},\text{Mrad}}$ , and  $\hat{Y}_{R,m=7}^{\mathcal{F},\text{prop},\text{Mrad}}$  are presented in Table 4. Estimators  $\hat{Y}_{R,m=7}^{\mathcal{F},\text{opt},\text{Mrad}}$ ,  $\hat{Y}_{R,m=3 \times 3 \times 3}^{\mathcal{F},\text{prop},\text{MRand3}}$ , and  $\hat{Y}_{R,m=3 \times 3 \times 3}^{\mathcal{F},\text{prop},\text{MHigh3}}$  are provided in Appendix A.4.6.

For  $t = -0.6$ , estimation of  $I$  from observations yielded 0, as the probability  $I = 0.001944$  is small, and none of the  $n = 500$  observations had all coordinates larger than  $t$ . Even in this case, the flow model captured the distribution well, yielding reasonable results – especially **MRand3** and **MHigh3** produced good

estimates ( $E=0.001913$ ). In one case, CMC yielded the best accuracy; in all other cases, stratified methods provided the best results.

Table 4: (Example 5) Results for Mrad, MHigh3 and MRand3 methods. Part 1

$f$	$I^*$	$\hat{Y}_{n=500}^{\text{obs}}$			$R$	$\hat{Y}_R^{\mathcal{F},\text{CMC}}$			$\hat{Y}_{R,m=3}^{\mathcal{F},\text{prop},\text{Mrad}}$			$\hat{Y}_{R,m=3}^{\mathcal{F},\text{opt},\text{Mrad}}$			$\hat{Y}_{R,m=7}^{\mathcal{F},\text{prop},\text{Mrad}}$		
		E*	SD*	AC		E*	SD*	AC	E*	SD*	AC	E*	SD*	AC	E*	SD*	AC
$j_{-1.0}^+$	1.37	1.80	.595	.504	$2^{12}$	1.67	.200	.733	1.52	.191	<b>1.18</b>	1.56	.191	<u>.832</u>	1.63	.197	.771
					$2^{13}$	1.67	.141	.703	1.71	.143	.633	1.71	.145	.683	1.66	.141	.686
$j_{-0.8}^+$	.560	.400	.282	.543	$2^{12}$	.735	.133	.635	.681	.128	<b>1.05</b>	.477	.089	.768	.662	.126	<u>1.01</u>
					$2^{13}$	.711	.092	.589	.669	.089	.807	.590	.082	<u>.936</u>	.655	.089	.777
$j_{-0.6}^+$	.194	.000	.000	.000	$2^{12}$	.236	.075	<b>1.00</b>	.227	.073	.683	.170	.057	.691	.227	.073	.805
					$2^{13}$	.267	.056	.506	.250	.055	.613	3.45	.029	.278	.238	.053	.784

**Model architecture and training details.** The CNF component of our model follows the FFJORD architecture [6], and our implementation is based on the original code. We use two stacked CNF blocks, each composed of two concat-squash layers with tanh activations and batch normalization. The number of hidden units (`dims`) depends on the example: 16 units for Examples A1 and 2, 64 units for Examples 1 and 4, 256 units for Examples 3 and 6, and 128 units for Example 5. The models are trained with the ADAM optimizer, using learning rates between 0.0001 and 0.01 and between several hundred and 5000 epochs, depending on the example.

## 5 Comprehensive Comparison

For Example 1, we conducted two additional comparisons. First, using the same training observations, we trained GMMs with 4, 10, 20, 50, and 100 components (denoted as  $\text{GMM}(k)$ ), then sampled from the trained models and computed function estimations. Results are shown in Table 5.

Estimations from the flow model, denoted  $\hat{Y}_R^{\mathcal{F}_{1k}}$  in the Table 5, are the same as  $\hat{Y}_R^{\mathcal{F},\text{CMC}}$  from Table 1. As clearly seen, in all cases, the flow model has the best accuracy, often by a large margin from any GMM (in each row, the best accuracy is **bolded**, second-best is underlined; note that the column  $\hat{Y}_R^{\mathcal{F}_{5k}}$  is not considered here). We did not apply stratification in this comparison. With stratification, the flow model achieves even better accuracy (as evidenced in Table 1). It is worth noting that if the data distribution were a mixture of Gaussians, GMMs would yield better results. We also trained a flow model  $\hat{Y}^{\mathcal{F}_{5k}}$  on a training set of size 5000. The results are provided in Table 5 (gray column). The performance of  $\hat{Y}^{\mathcal{F}_{1k}}$  and  $\hat{Y}^{\mathcal{F}_{5k}}$  remains consistent, showing that 1000 points were *enough* to train the flow model accurately. More detailed model performance as the function training dataset size is further investigated in next section.

Table 5: (Example 2) Comparison with GMM and with flow model  $\mathcal{F}_{5k}$  trained on 5000 observations.

$f$	$I$	$R$	$\hat{Y}_R^{\mathcal{F}_{1k}}$		$\hat{Y}_R^{\mathcal{F}_{5k}}$		$\hat{Y}_R^{\text{GMM}(4)}$		$\hat{Y}_R^{\text{GMM}(10)}$		$\hat{Y}_R^{\text{GMM}(20)}$		$\hat{Y}_R^{\text{GMM}(50)}$		$\hat{Y}_R^{\text{GMM}(100)}$	
			E	AC	E	AC	E	AC	E	AC	E	AC	E	AC	E	AC
$j_{0.5}^+$	.315	$2^{12}$	.304	<b>1.68</b>	.321	1.72	.359	.857	.305	<u>1.54</u>	.306	1.22	.323	1.52	.335	1.20
		$2^{15}$	.307	<b>1.63</b>	.306	1.54	.355	.898	.319	<u>1.52</u>	.321	1.43	.327	1.41	.327	1.40
$j_{1.2}^+$	.032	$2^{12}$	.031	<b>1.25</b>	.025	1.68	.063	.019	.040	.060	.039	<u>.644</u>	.023	.557	.024	.569
		$2^{15}$	.032	<b>1.81</b>	.029	.882	.068	-.035	.040	.060	.038	<u>.796</u>	.022	.504	.024	.602
$j_{2.0}^+$	.001	$2^{12}$	.001	<b>.613</b>	.001	.945	.002	-.134	0	0	.000	<u>.388</u>	.000	.388	.002	.152
		$2^{15}$	.001	<b>.668</b>	.001	1.00	0.02	-0.13	.000	.130	.000	<u>.284</u>	.000	.089	.000	.109
$h_1$	.033	$2^{12}$	.031	<b>1.40</b>	.033	1.71	.052	.261	.050	.303	.042	.577	.037	<u>.966</u>	.038	.855
		$2^{15}$	.032	<b>1.51</b>	.032	1.51	.058	.131	.052	.251	.040	.723	.028	.776	.034	1.33
$h_2$	.032	$2^{12}$	.030	<b>1.35</b>	.031	1.71	.051	.272	.040	.588	.034	<u>1.14</u>	.034	1.07	.040	.064
		$2^{15}$	.031	<b>1.50</b>	.029	.998	.054	.154	.052	.251	.034	<u>1.22</u>	.034	1.21	.035	.957
$h_3$	.123	$2^{12}$	.112	<b>1.08</b>	.118	1.14	.185	.296	.139	.894	.112	<u>1.05</u>	.148	.698	.158	.551
		$2^{15}$	.122	<b>1.53</b>	.116	1.41	.185	.296	.160	.525	.132	<u>1.14</u>	.132	1.12	.139	.882

## 6 Sample size performance

Fig. 4 illustrates the accuracy of estimating  $I = \mathbb{E} f(\mathbf{X})$  from Example 1 using samples generated from a normalizing flow trained on datasets of varying size  $n_{\text{train}}$ .

Horizontal lines represent the true values of  $I$ , while the curves correspond to flow-based estimates. The results show that already for training samples of several hundreds, the flow achieves sufficient accuracy and the estimates stabilize around the true values (cf. Table 1).

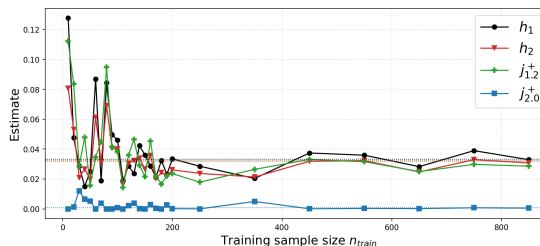


Fig. 4: Estimates vs. training sample size  $n_{\text{train}}$ .

## 7 Related work

The scenario where the distribution of  $\mathbf{X}$  is known, and the goal is to construct an estimator of (1) with reduced variance using a neural network, has been studied in the literature. For example, the **control variates** variance reduction technique, which aims to find a family of functions  $g$  for which  $\mathbb{E} g(\mathbf{X}) = 0$ , was investigated in [11]. In [21], the authors proposed *neural control variates* (NCV), where  $g$  is designed as a neural network. A similar approach (with applications in light transport for computer vision), using a normalizing flow for  $g$ , was studied in [13]. An application of Stein’s identity to control variates, where  $g$  can be a neural network, was presented in [9]. Another commonly used method in the context of integration is the **importance sampling** variance reduction technique. In [12],

the authors used a nonlinear independent components estimation (NICE) flow model [4] to learn a simple variational distribution.

Stratified sampling has also been used to estimate (1) with normalizing flows. In [3], the authors tackle a slightly different problem—estimating high-dimensional integrals and controlling the bias-variance trade-off by interpolating between sampling and variational regimes. They employed the RealNVP model [5] with a uniform base distribution. Spherical stratification with adaptive radial splitting was used in [18].

Estimating the expectation of a real-valued function of a random variable using only observations has been studied in the context of learning tail behavior. The ability of popular normalizing flow models to capture tail probabilities was examined in [7], where the authors propose tail-adaptive flows, which perform better for non-Gaussian tails. This work is extended in [8], where the authors allow for heavy-tailed base distributions on selected coordinates.

## 8 Conclusions and limitations

We introduce a flow-based model that uses a parametrized neural network, allowing for greater flexibility in modeling unknown data distributions. Our approach is validated in the context of stratified sampling and outperforms traditional methods in reducing estimation uncertainty on both synthetic and real-world datasets, including high-dimensional cases. Overall, this work offers a promising path for improving the accuracy and reliability of statistical data analysis. In future work, we plan to evaluate the approach across a wide range of real-life applications. One limitation is that the normalizing flow used is less accurate for heavy-tailed data distributions. Additionally, the model requires training, which can be time-consuming.

**Training time.** Training times are available in Appendix A.5.

**Future work.** An in-depth study of alternative flow base distributions (e.g., those capable of modeling heavy-tailed distributions) and methods for **choosing strata** (note that the optimal split  $R_1, \dots, R_m$  presented in Section 2.3 is for *given* strata) are left for future work. In Appendix A.6, we present preliminary results for a method that “rotates” spherical strata based on the estimated function to improve estimation. For example, rotating the strata from Fig. 3 (right) by  $29.33^\circ$  (see the corresponding figure in Appendix A.6) yields better estimations.

## References

1. R. Abdal, P. Zhu, N. J. Mitra, and P. Wonka. Styleflow: Attribute-conditioned exploration of stylegan-generated images using conditional continuous normalizing flows. *ACM Transactions on Graphics (ToG)*, 40(3):1–21, 2021.
2. A. X. Chang, T. Funkhouser, L. Guibas, P. Hanrahan, Q. Huang, Z. Li, S. Savarese, M. Savva, S. Song, H. Su, et al. Shapenet: An information-rich 3d model repository. *arXiv preprint arXiv:1512.03012*, 2015.

3. C. Cundy and S. Ermon. Flexible approximate inference via stratified normalizing flows. In *Conference on Uncertainty in Artificial Intelligence*, pages 1288–1297. PMLR, 2020.
4. L. Dinh, D. Krueger, and Y. Bengio. NICE: non-linear independent components estimation. In Y. Bengio and Y. LeCun, editors, *3rd International Conference on Learning Representations, ICLR 2015, San Diego, CA, USA, May 7-9, 2015, Workshop Track Proceedings*, 2015.
5. L. Dinh, J. Sohl-Dickstein, and S. Bengio. Density estimation using real NVP. In *5th International Conference on Learning Representations, ICLR 2017, Toulon, France, April 24-26, 2017, Conference Track Proceedings*. OpenReview.net, 2017.
6. W. Grathwohl, R. T. Q. Chen, J. Bettencourt, I. Sutskever, and D. Duvenaud. FFJORD: free-form continuous dynamics for scalable reversible generative models. In *7th International Conference on Learning Representations, ICLR 2019, New Orleans, LA, USA, May 6-9, 2019*. OpenReview.net, 2019.
7. P. Jainsi, I. Kobzyev, Y. Yu, and M. Brubaker. Tails of lipschitz triangular flows. In *International Conference on Machine Learning*, pages 4673–4681. PMLR, 2020.
8. M. Laszkiewicz, J. Lederer, and A. Fischer. Marginal tail-adaptive normalizing flows. In *ICML*, pages 12020–12048. PMLR, 2022.
9. H. Liu, Y. Feng, Y. Mao, D. Zhou, J. Peng, and Q. Liu. Action-depedent control variates for policy optimization via stein’s identity. *arXiv preprint arXiv:1710.11198*, 2017.
10. N. Madras. *Lectures on Monte Carlo methods*, volume 16. American Mathematical Soc., 2002.
11. A. Mira, R. Solgi, and D. Imparato. Zero variance markov chain monte carlo for bayesian estimators. *Statistics and Computing*, 23:653–662, 2013.
12. T. Müller, B. McWilliams, F. Rousselle, M. Gross, and J. Novák. Neural importance sampling. *ACM Transactions on Graphics (ToG)*, 38(5):1–19, 2019.
13. T. Müller, F. Rousselle, A. Keller, and J. Novák. Neural control variates. *ACM Transactions on Graphics (TOG)*, 39(6):1–19, 2020.
14. PointFlow. PointFlow : 3D Point Cloud Generation with Continuous Normalizing Flows. Github repository. <https://github.com/stevenygd/PointFlow/>, 2019.
15. D. Rezende and S. Mohamed. Variational inference with normalizing flows. In *ICML*. PMLR, 2015.
16. SDF. Simple SDF mesh generation in Python. Github repository. [github.com/fogleman/sdf/](https://github.com/fogleman/sdf/), 2021.
17. M. Sendera, J. Tabor, A. Nowak, A. Bedychaj, M. Patacchiola, T. Trzciński, P. Spurek, and M. Zięba. Non-gaussian gaussian processes for few-shot regression. In *Advances in Neural Information Processing Systems*, 2021.
18. C. Song and R. Kawai. Adaptive radial importance sampling under directional stratification. *Probabilistic Engineering Mechanics*, 72:103443, 2023.
19. E. G. Tabak and E. Vanden-Eijnden. Density estimation by dual ascent of the log-likelihood. *Communications in Mathematical Sciences*, 8(1):217–233, 2010.
20. AmeriGEOSS. Wind-measurements in Papua New Guinea, 2019. data retrieved from <https://data.amerigeoss.org/dataset/857a9652-1a8f-4098-9f51-433a81583387/resource/a8db6cec-8faf-4c8e-aee2-4fb45d1e6f14>.
21. R. Wan, M. Zhong, H. Xiong, and Z. Zhu. Neural control variates for variance reduction. *arXiv preprint arXiv:1806.00159*, 2018.
22. G. Yang, X. Huang, Z. Hao, M.-Y. Liu, S. Belongie, and B. Hariharan. Pointflow: 3d point cloud generation with continuous normalizing flows. In *Proceedings of*

16 P. Lorek, R. Nowak, R. Topolnicki, T. Trzcinski, M. Zięba, A. Krystecka

*the IEEE/CVF International Conference on Computer Vision*, pages 4541–4550,  
2019.

## A.1 More on stratified sampling

As mentioned, the proof of Theorem A1 and the decomposition of a variance of CMC estimator may be found e.g., in Madras (Theorem 3.3). In next two subsections we provide different proofs of those.

### A.1.1 Variance decomposition

Recall that  $I = \mathbb{E}Y$  and that expectation of  $I$  on  $j$ -th strata was defined as  $I^j = \mathbb{E}[Y|Y \in A^j]$ . Define a random variable  $J(\omega) = j$  iff  $\omega \in A^j$ . We have

$$\begin{aligned} \mathbb{E} \text{Var}(Y|J) &= \sum_{j=1}^m p_j \text{Var}(Y|J=j) = \sum_{j=1}^m p_j \sigma_j^2, \\ \text{Var} \mathbb{E}(Y|J) &= \mathbb{E}(\mathbb{E}(Y|J) - \mathbb{E}(\mathbb{E}(Y|J)))^2 = \mathbb{E}(\mathbb{E}(Y|J) - EY)^2 \\ &= \mathbb{E}(\mathbb{E}(Y|J) - I)^2 = \sum_{j=1}^m (E(Y|J=j) - I)^2 = \sum_{j=1}^m p_j (I^j - I)^2. \end{aligned}$$

Using the *law of total variance*  $\text{Var} Y = \mathbb{E} \text{Var}(Y|J) + \text{Var} \mathbb{E}(Y|J)$ , we may decompose a variance into **within** and **between-stratum** components given in (A1), i.e.,

$$\text{Var} Y = \sum_{j=1}^m p_j \sigma_j^2 + \sum_{j=1}^m p_j (I^j - I)^2. \quad (\text{A1})$$

In below computations we ignore issues with roundings – e.g., in practice we take  $R_j = \lceil R p_j \rceil$ .

**Lemma 1.** *We have a following decomposition of a variance of CMC estimator involving variance of proportional allocation estimator:*

$$\text{Var}(\hat{Y}_R^{\text{CMC}}) = \text{Var}(\hat{Y}_R^{\text{pa}}) + \frac{1}{R} \sum_{j=1}^m p_j (I^j - I)^2 \geq \text{Var}(\hat{Y}_R^{\text{pa}}).$$

*Proof.* Let us introduce the following notation. For  $\mathbf{x} = (x_1, \dots, x_m)$  (here  $x_i > 0$  and  $x_1 + \dots + x_m = 1$ ) define

$$\sigma_{\text{str}}^2(\mathbf{x}) := \sum_{i=1}^m \frac{p_i^2}{x_i} \sigma_i^2. \quad (\text{A2})$$

In proportional allocation we have  $R_j = p_j R$ , thus

$$\text{Var}(\hat{Y}_R^{\text{pa}}) = \frac{1}{R} \sigma_{\text{str}}^2(R_1/R, \dots, R_m/R) = \frac{1}{R} \sum_{j=1}^m p_j \sigma_j^2.$$

Dividing both sides of (A1) we have

$$\frac{1}{R} \text{Var} Y = \frac{1}{R} \sum_{j=1}^m p_j \sigma_j^2 + \frac{1}{R} \sum_{j=1}^m p_j (I^j - I)^2$$

i.e.,

$$\text{Var}(\hat{Y}_R^{\text{CMC}}) = \text{Var}(\hat{Y}_R^{\text{pa}}) + \frac{1}{R} \sum_{j=1}^m p_j (I^j - I)^2.$$

### A.1.2 Optimal allocation – proof

Let us start with describing an intuition on why the proportional allocation may not be optimal: for some strata  $A^j$  we may have that the variability (sample variance) of replications of  $Y^j$  is smaller than the variability of replications of  $Y^{j'}$  sampled from strata  $A^{j'}$ . It is reasonable to “spend” more replications for strata  $A^{j'}$  than  $A^j$ . The following theorem makes this intuition precise and provides the best possible (for fixed strata) split of  $R$ .

**Theorem A1.** *Let  $m$  strata  $A^1, \dots, A^m$  and total budget  $R$  of simulations be fixed. Let  $\hat{Y}_R^{\text{str}}$  be a stratified estimator with a general split, whereas let  $\hat{Y}_R^{\text{opt}}$  be the stratified estimator with optimal split*

$$R_j = \frac{p_j \sigma_j}{\sum_{i=1}^m p_i \sigma_i} R, \quad j = 1, \dots, m. \quad (\text{A3})$$

Then we have  $\text{Var}(\hat{Y}_R^{\text{opt}}) \leq \text{Var}(\hat{Y}_R^{\text{str}})$ .

*Proof.* We may rewrite rhs of variance given in (2.3) as

$$\frac{1}{R} \left( p_1^2 \frac{R}{R_1} \sigma_1^2 + \dots + p_m^2 \frac{R}{R_m} \sigma_m^2 \right) = \frac{1}{R} \left( \frac{p_1^2}{R_1/R} \sigma_1^2 + \dots + \frac{p_m^2}{R_m/R} \sigma_m^2 \right) \quad (\text{A4})$$

$$= \frac{1}{R} \sigma_{\text{str}}^2((R_1/R, \dots, R_m/R)). \quad (\text{A5})$$

Denote  $D = \sum_{j=1}^m p_j \sigma_j$ . The stratified estimator with split given in (A3), i.e., with  $R_i = \frac{p_i \sigma_i}{D} R$  is denoted by  $\hat{Y}_R^{\text{opt}}$ . Recalling (A4), using (A2) and  $R_i/R = \frac{p_i \sigma_i}{D}$  we have

$$\text{Var} \hat{Y}_R^{\text{opt}} = \frac{1}{R} \sigma_{\text{str}}^2((R_1/R, \dots, R_m/R)) = \frac{1}{R} \sum_{j=1}^m \frac{p_j^2}{p_j \sigma_j / D} \sigma_j^2 = \frac{1}{R} D \sum_{j=1}^m p_j \sigma_j = \frac{1}{R} D^2.$$

Let  $\hat{Y}_R^{\text{str}}$  be some general stratified estimator with  $R_i = x_i R$ , where  $x_1 + \dots + x_m = 1, x_j \geq 0$ . Denote  $\mathbf{x} = (x_1, \dots, x_m)$ . Let

$$\boldsymbol{\gamma}^* = (\gamma_1^*, \dots, \gamma_m^*), \quad \gamma_j^* = \frac{p_j \sigma_j}{D}.$$

Using Cauchy-Schwarz inequality, for any  $\mathbf{x}$  such that  $x_1 + \dots + x_m = 1, x_j > 0$  we have

$$\begin{aligned} \text{Var} \hat{Y}_R^{\text{opt}} &= \frac{1}{R} D^2 = \frac{1}{R} \left( \sum_{j=1}^m p_j \sigma_j \right)^2 = \frac{1}{R} \left( \sum_{j=1}^m \sqrt{x_j} \frac{p_j \sigma_j}{\sqrt{x_j}} \right)^2 \\ &\leq \frac{1}{R} \sum_{k=1}^m x_k \sum_{j=1}^m \frac{p_j^2 \sigma_j^2}{x_j} = \frac{1}{R} \sum_{j=1}^m \frac{p_j^2}{x_j} \sigma_j^2 = \frac{1}{R} \sigma_{\text{str}}^2(\mathbf{x}) = \text{Var} \hat{Y}_R^{\text{str}}, \end{aligned}$$

thus, the variance is minimal for  $\mathbf{x} = \gamma^*$ .

## A.2 Spherical stratification w.r.t. to angles

In Section 3.1 we shortly pointed out how to perform spherical stratification w.r.t. angles. Recall, the main idea is to sample the point uniformly from sphere the hypersphere

$$S_{d-1} = \left\{ \mathbf{x} = (x_1, \dots, x_d) : \sum_{j=1}^d x_j^2 = 1 \right\}.$$

Note that a point  $\mathbf{x} \in S_{d-1}$  has spherical coordinates

$$\begin{aligned} x_1 &= \cos \phi_1, & x_2 &= \sin \phi_1 \cos \phi_2, \dots, \\ x_d &= \sin \phi_1 \cdots \sin \phi_{d-3} \sin \phi_{d-2} \sin \theta, \end{aligned}$$

where  $\phi_1, \dots, \phi_{d-2} \in [0, \pi)$  and  $\theta \in [0, 2\pi)$ . The transformation between Cartesian and spherical coordinates has Jacobian

$$J(\phi_1, \dots, \phi_{d-2}, \theta) = \sin^{d-2} \phi_1 \sin^{d-3} \phi_2 \cdots \sin \phi_{d-2}.$$

The area of  $S_{d-1}$  is  $2\pi^{d/2}/\Gamma(d/2)$ , thus the density of a uniform distribution on  $S_{d-1}$  is

$$g(\theta, \phi_1, \dots, \phi_{d-2}) = \frac{\Gamma(d/2)}{2\pi^{d/2}} \sin^{d-2} \phi_1 \sin^{d-3} \phi_2 \cdots \sin \phi_{d-2}. \quad (\text{A6})$$

Using the identity  $c_k = \int_0^\pi \sin^k(x) dx = B\left(\frac{1}{2}, \frac{k+1}{2}\right)$ , where  $B(a, b)$  is a beta function, one may decompose (A6) into

$$\frac{1}{2\pi} \prod_{k=2}^{d-1} \frac{1}{c_{d-k}} \sin^{d-k}(\phi_{k-1}) = h_0(\theta) \prod_{k=2}^{d-1} h_{d-k}(\phi_{k-1}),$$

where  $h_0$  is a density of the uniform distribution on  $(0, 2\pi)$  and

$$h_k(\phi) = \frac{1}{c_k} \sin^k(\phi), \phi \in (0, 2\pi), \quad c_k = \int_\pi \sin^k(x) dx = B\left(\frac{1}{2}, \frac{k+1}{2}\right),$$

Since we have a product, it means that we may sample from a uniform distribution on  $S_{d-1}$  by sampling  $\theta, \phi_1, \dots, \phi_{d-2}$  with distributions  $h_0, h_1, \dots, h_{d-2}$  correspondingly. sampling from  $h_k$  for general  $k$  is not straightforward, mainly because there is no closed formula for  $\int_0^t \sin^k(x) dx$  and thus for a distribution function of  $h_k$  (what would allow for using an inverse method). We will use **acceptance-rejection** (AR) method. Recall, to sample from  $h_k(x)$  we may sample from another density  $q_k(x)$  (also on  $(0, \pi)$ ) assuming we know a constant  $C_k$  such that  $h_k(x) \leq C_k q_k(x)$ . We may simply take  $q_k(x)$  to be a uniform distribution on  $(0, \pi)$ , i.e.,  $q_k(x) = 1/\pi$ . Since  $h_k(x) = c_k \sin^k(x) \leq c_k$ , we may

simply take  $C_k = \pi/c_k$ . Finally, the procedure is as follows: We generate  $U, U'$  iid  $\mathcal{U}(0, 1)$ , set  $T = U'\pi$  and accept it if  $C_k U/\pi \leq h_k(T)$  (note that it may be simplified to  $U \leq \sin^k(T)$ ). We repeat the procedure until acceptance. The procedure is provided in Algorithm 1. Note that line 5 can be simplified to: **until**  $U \leq \sin^k(T)$ .

---

**Algorithm 1** AR Algorithm for sampling from  $h_k$ .

---

**Require:** constant  $c_k$

- 1: Set  $C_k = \pi/c_k$
  - 2: **repeat**
  - 3:   Generate  $U' \sim \mathcal{U}(0, 1)$  and set  $T = U'\pi$
  - 4:   Generate  $U \sim \mathcal{U}(0, 1)$  (independent from  $U'$ )
  - 5: **until**  $C_k U/\pi \leq h_k(T)$  **return**  $T$
- 

To conduct **stratified sampling** we proceed with AR algorithm with the change that we sample  $U'$  from some strata (5), where  $a_0 = 0, a_{m_0} = 1$  and  $a_j, j = 1 \dots, m_0 = 1$  are chosen so that the strata are equally likely, i.e.,  $\frac{1}{c_k} \int_{a_{j-1}}^{a_j} \sin^k(x) dx = \frac{1}{m_0}$ . Values of  $a_j$  are found by numerical integration.

**Expected running time of AR Algorithm 1.** Acceptance-rejection expected running time is  $C_k$ , which is  $\pi/c_k$ . For example for  $k = 10$  (recall that  $k$  is at most  $d - 2$ ) on average  $C_{10} = \pi/.7731 = 4.063$  iterations of AR are needed (to sample one random point), whereas e.g., for  $k = 200$  on average  $C_{200} = \pi/.1770 = 17.746$  iterations are needed. Thus, in practice, the running time of AR algorithm is not problematic.

### A.3 Details on high-dimensional stratification

We aim to sample multivariate standard normal vector  $(Z_1, \dots, Z_d)$  in a stratify way using  $m$  equally likely strata. The cartesian method M1 splits each coordinates into  $m_0$  strata, see Eq. (5). The spherical method M2 splits radius into  $m_r$  strata and each angle into  $m_0$  strata. Thus, if decide to split each dimension in M1 method into  $m_0 = 2$  strata or each angle into  $m_0 = 2$  strata, we have exponential  $(2^d, m_r 2^d)$  number of total strata, which is prohibitive for large  $d$  (in our Examples 5 and 6 we had  $d = 30$  and  $d = 128$  respectively). Here we describe two methods mitigating this problem.

#### A.3.1 Mrad method: stratification w.r.t radius

This is a special case of the spherical method: independently of  $d$ , in spherical method we may decide to stratify only w.r.t radius  $D$ . We thus set  $m = m_r > 1$  and  $m_0 = 1$  and perform the procedure described in the first paragraph of section 3.1. In other words, we split

$$\mathbb{R}^d = A^1 \cup A^2 \cup \dots \cup A^m$$

into  $m$  equally probable strata (e.g., in Fig. 3 top-right we have  $m = 4$  strata if we disregard splitting w.r.t angles). Sampling multivariate standard normal random vector from strata  $A^j$ , i.e.,

$$\mathbf{Z}^j \stackrel{\mathcal{D}}{=} (\mathbf{Z} | \mathbf{Z} \in A^j)$$

is given by the procedure:

- sample  $\mathbf{Z} = (Z_1, \dots, Z_d)$  with  $d$  iid standard normal  $\mathcal{N}(0, 1)$  random variables,
- normalize  $\mathbf{Z}$  to get  $\mathbf{Z}' = \left( \frac{Z_1}{\|\mathbf{Z}\|}, \dots, \frac{Z_d}{\|\mathbf{Z}\|} \right)$ ,
- sample  $U \sim \mathcal{U}(0, 1)$ ,
- Compute  $(D^j)^2 = F_{\chi_d^2}^{-1} \left( \frac{j}{m_r} + \frac{1}{m_r} U \right)$ ,
- Set  $\mathbf{Z}^j = (D^j Z'_1, \dots, D^j Z'_d)$ .

We denote the resulting estimators as  $\hat{Y}_{R, m_r=m}^{\mathcal{F}, \text{opt}, \text{Mrad}}$  (proportional allocation) and  $\hat{Y}_{R, m_r=m}^{\mathcal{F}, \text{opt}, \text{Mrad}}$  (optimal allocation). Note that the method does not depend on a function  $f$  we aim to estimate (recall, the goal is to estimate  $I = \mathbb{E} f(\mathbf{X})$ ).

### A.3.2 MHigh3 and MRand3 methods: stratifying three chosen coordinates

Using an obvious decomposition  $\mathbb{R}^d = \mathbb{R} \times \mathbb{R} \dots \times \mathbb{R}$  ( $d$  times), we will split  $\eta = 3$  chosen *dimensions* (coordinates) into  $m_0$  strata, obtaining thus in total  $m = m_0^3$  strata. Say, the chosen dimensions (we describe below how to choose them) are  $i, j, k$ . Let each  $A_i^s, A_j^s, A_k^s, s = 1, \dots, m_0$  be the a split of  $\mathbb{R}$  into  $m_0$  intervals, such that  $\mathbb{P}(Z \in A_i^s) = 1/m_0$ , i.e., as it was given in (5):

$$\begin{aligned} A_i^1 &= (a_0, a_1], \dots, A_i^{m_0} = (a_{m_0-1}, a_{m_0}], \\ A_j^1 &= (a_0, a_1], \dots, A_j^{m_0} = (a_{m_0-1}, a_{m_0}], \\ A_k^1 &= (a_0, a_1], \dots, A_k^{m_0} = (a_{m_0-1}, a_{m_0}], \end{aligned}$$

where

$$a_0 = -\infty, \quad a_1 = \Phi^{-1} \left( \frac{1}{m_0} \right), \quad a_2 = \Phi^{-1} \left( \frac{2}{m_0} \right), \quad \dots, \quad a_{m_0} = \infty.$$

Denoting  $(A_i^{s_i}, A_j^{s_j}, A_k^{s_k})$  are on coordinates  $i, j, k$

$$A_{ijk}^{s_i, s_j, s_k} = \mathbb{R} \times \mathbb{R} \times \dots \times A_i^{s_i} \times \mathbb{R} \dots \times A_j^{s_j} \times \mathbb{R} \dots \times A_k^{s_k} \times \mathbb{R} \dots \times \mathbb{R}$$

we have  $\mathbb{P}(\mathbf{Z} \in A_{ijk}^{s_i, s_j, s_k}) = 1/(m_0^3) = 1/m$ . In other words, we stratified  $\mathbb{R}^d$  into disjoint equally probable regions

$$\mathbb{R}^d = \bigcup_{(s_i, s_j, s_k) \in \{1, \dots, m_0\}^d} A_{ijk}^{s_i, s_j, s_k}.$$

Sampling  $\mathbf{Z} = (Z_1, \dots, Z_d)$  from strata  $A_{ijk}^{s_i, s_j, s_k}$  is straightforward: we sample  $Z_t \sim \mathcal{N}(0, 1)$  for  $t \notin \{i, j, k\}$  and sample  $Z_i$  from  $A_i^{s_i}$ ,  $Z_j$  from  $A_j^{s_j}$  and  $Z_k$  from  $A_k^{s_k}$  as described in section 3.1. For example, to sample  $Z_i$  from  $A_i^{s_i}$  we sample  $U \sim \mathcal{U}(0, 1)$  and set

$$Z_i = \Phi^{-1}(V^{s_i}), \quad \text{where } V^{s_i} = a_{s_i-1} + (a_{s_i} - a_{s_i-1})U.$$

The way of choosing  $i, j, k$  determines the method.

- **Method MRand3.** We simply choose (different)  $i, j, k$  uniformly at random from  $\{1, \dots, d\}$ .
- **Method MHigh3.** Here, the choice depends on a final function we are to estimate ( $I = \mathbf{E} f(\mathbf{X})$ ). First, we separately consider stratification w.r.t to one dimension only, i.e., we fix  $b$  and consider stratification

$$\mathbb{R}^d = \bigcup_{s=1}^{m_0} A_{b,s}, \quad \text{where } A_{b,s} = \mathbb{R} \times \dots \times \mathbb{R} \times \underbrace{A_b^s}_{b\text{-th dimension}} \times \mathbb{R} \times \dots \times \mathbb{R}.$$

Here  $A_i^s = (a_{s-1}, a_s)$ .

Now we perform  $R_0 < R$  pilot simulations and use stratification with proportional allocation to obtain the estimator  $\hat{Y}_{R_0}^{\mathcal{F}, \dim=b}$ . Denote its standard deviation by  $\sigma^{\dim=b} = \sqrt{\text{Var} \hat{Y}_{R_0}^{\mathcal{F}, \dim=b}}$ . Now we consider three different  $b$ 's for which  $\sigma^{\dim=b}$  were largest – we take these as  $i, j, k$ .

Note that MRand and MRand3 do not depend on  $f$ , whereas MHigh3 does. All our experiments were done for  $\eta = 3$  chosen coordinates, of course it may be other number – it must be relatively small so that total number of strata  $m_0^\eta$  is not prohibitive. Recall also that in all experiments we present averages from 10 simulations. In particular, for method MRand3, in each simulation  $i, j, k$  were sampled independently.

## A.4 More details on experimental results

**Model architecture and training details.** The CNF component for our model was inspired by FFJORD. Our implementation is based on the original code provided by the authors. We use two stacked blocks of CNFs, each composed of two hidden concatsquash layers, 16 units (`dims`) (Example A1 and 2), 64 units (Example 1 and 4), 256 units (Example 3 and 6) or 128 units (Example 5) each, with  $\tanh(\cdot)$  activation. After each of the units, we apply the batch-norm operation. We train the model using an ADAM optimizer with a learning rate

---

<https://github.com/rtqichen/ffjord>

ranging from 0.0001 to 0.01 and number of epochs ranging from several hundreds to 5000 (depending on example, details can be checked in code).

**Remark.** In all tables presented in this appendix that consist of parts (a) and (b), the highlighting conventions (**bold** for the best value and underlined for the second best) are applied jointly across both parts, i.e., comparisons are made between all rows appearing in (a) and (b).

### A.4.1 Example 1

We provide here more numerical results. Recall, in Table 1 we provided results for cartesian stratification, for selected model – in Table A1 we provide results for more models including both, AC and SD\*. Moreover, in Table A2 we provide results for spherical stratification.

To compare only stratification methods – values of AC from Tables 1 and A2 (only for  $R = 2^{12}$ ) are collected in Table A3. Note that there is no clear “winner”. Out of 24 pairs (cartesian vs spherical) cartesian stratification is better in 13 cases. However, considering only the best accuracy in each of rows (i.e., for each function), spherical stratification is better in 4 cases.

Table A3: Example A1: Comparison of accuracy AC of cartesian (M1) and spherical (M2) stratification for  $R = 2^{12}$ . Data from Tables 1 and A2. Best accuracy in each pair (M1, M2) is underlined, best accuracy in a whole row is **bolded**.

$t$	$\hat{Y}_{R,m=2 \times 2}^{\mathcal{F},\text{prop}}$		$\hat{Y}_{R,m=2 \times 2}^{\mathcal{F},\text{opt}}$		$\hat{Y}_{R,m=4 \times 4}^{\mathcal{F},\text{prop}}$		$\hat{Y}_{R,m=4 \times 4}^{\mathcal{F},\text{opt}}$	
	M1 (cart)	M2 (spher)	M1 (cart)	M2 (spher)	M1 (cart)	M2 (spher)	M1 (cart)	M2 (spher)
$j_{0.5}^+$	1.576	<b>1.654</b>	1.537	<u>1.619</u>	<u>1.651</u>	1.622	1.568	<u>1.662</u>
$j_{1.2}^+$	1.837	<u>1.889</u>	<b>2.144</b>	1.992	<u>1.846</u>	1.745	<u>2.216</u>	1.880
$j_{2.0}^+$	.6904	<b>.9075</b>	<u>.7675</u>	.5958	<u>.9000</u>	.7266	.6933	.6534
$h_1$	1.330	<b>1.580</b>	1.456	<u>1.531</u>	<u>1.548</u>	1.355	1.463	<u>1.579</u>
$h_2$	1.488	<b>1.601</b>	<u>1.597</u>	1.437	<u>1.549</u>	1.483	1.471	<u>1.505</u>
$h_3$	<u>1.613</u>	1.546	1.622	<u>1.679</u>	<u>1.656</u>	1.403	<b>1.829</b>	1.739

In Fig. 1 we presented confidence intervals resulting from 100 iterations of the whole procedure (recall, in all the tables average of 10 simulations is reported) for estimating  $I = \mathbb{P}(X_1 > 1.2, X_2 > 1.2)$  (i.e.,  $\mathbb{E}j_{1.2}^+(\mathbf{X})$ ) using  $R = 2^{12}$  replications, we presented plots only for  $\hat{Y}_R^{\mathcal{F},\text{CMC}}$  and  $\hat{Y}_{R,m=16}^{\mathcal{F},\text{opt},\text{M1}}$  (i.e., cartesian stratification). Fig. A1 is an extended version of Fig. 1, it also contains  $\hat{Y}_{R,m=4}^{\mathcal{F},\text{prop},\text{M1}}$ ,  $\hat{Y}_{R,m=4}^{\mathcal{F},\text{opt},\text{M1}}$  and  $\hat{Y}_{R,m=16}^{\mathcal{F},\text{prop},\text{M1}}$  estimators. Fig. A2 contains similar confidence intervals computed from simulations involving spherical stratification (note that  $\hat{Y}_R^{\mathcal{F},\text{CMC}}$  used the same randomness in both cases). To be more precise, for  $i = 1, \dots, 100$  we perform the sampling procedure, estimate the value of  $I$  via  $\hat{Y}_R^{(i)}$  (one of: CMC or some stratified estimator) and compute  $\text{Var}(\hat{Y}_R^{(i)})$ .

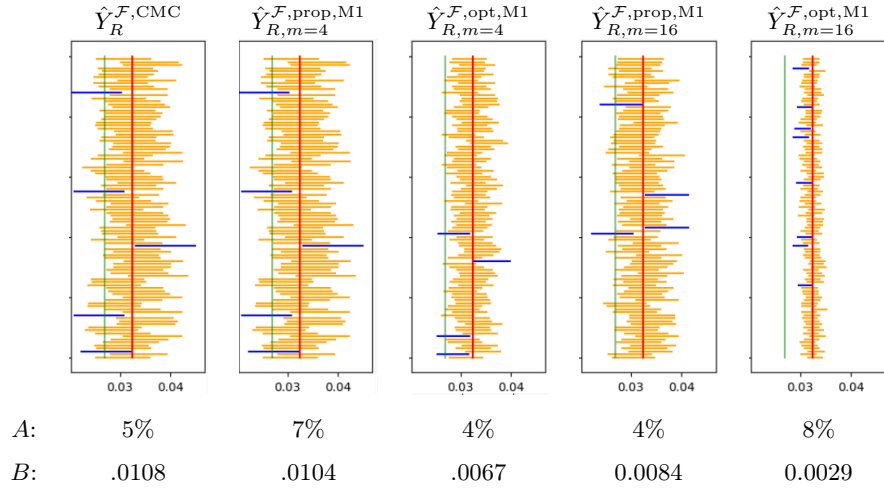


Fig. A1: Example A1: 100 estimations of  $I = \mathbb{P}(X_1 > 1.2, X_2 > 1.2)$ , each from  $R = 2^{12}$  simulations. 95% confidence intervals depicted. Red line – true  $I$ , green line –  $\hat{Y}_n^{\text{obs}}$ , orange lines – intervals containing  $I$ ; blue lines: those not containing  $I$ . A: percentage of intervals not containing  $I$ ; B: average confidence interval length

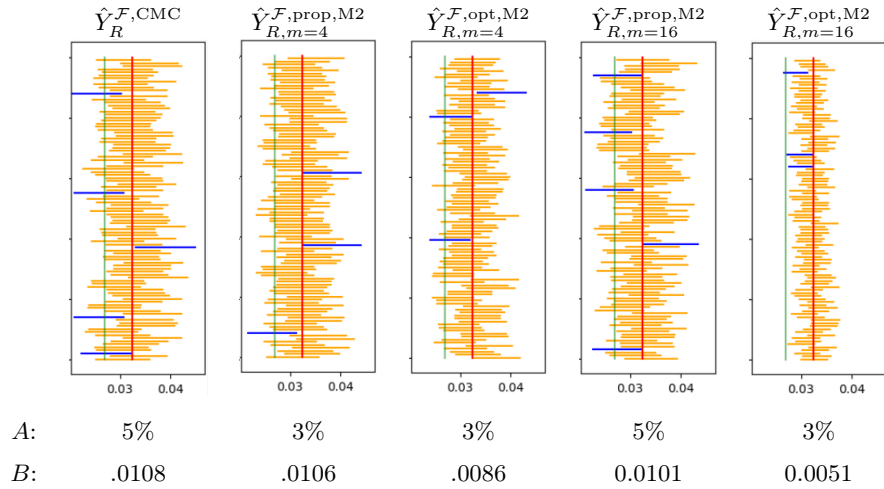


Fig. A2: Example A1:  $R = 2^{12}$ , spherical stratification, 100 hundred estimations of  $I = \mathbb{P}(X_1 > 1.2, X_2 > 1.2)$ . Confidence interval (at significance lever  $\alpha = 5\%$ ) depicted. Red line – true  $I$ , green line –  $\hat{Y}_n^{\text{obs}}$ , orange lines – intervals containing  $I$ ; blue lines: those not containing  $I$ . A: percentage of intervals not containing  $I$ ; B: average confidence interval length

Afterwards, we draw intervals

$$\left[ \hat{Y}_R^{(i)} - z_{1-\alpha/2} \text{Var}(\hat{Y}_R^{(i)}), \hat{Y}_R^{(i)} + z_{1-\alpha/2} \text{Var}(\hat{Y}_R^{(i)}) \right].$$

The theory states that

$$\mathbb{P} \left( I \in \left[ \hat{Y}_R^{(i)} - z_{1-\alpha/2} \text{Var}(\hat{Y}_R^{(i)}), \hat{Y}_R^{(i)} + z_{1-\alpha/2} \text{Var}(\hat{Y}_R^{(i)}) \right] \right) \approx 1 - \alpha.$$

All the figures are for  $\alpha = 5\%$ , which means that 5% of confidence intervals does not contain (on average) a true value of  $I$ . More precisely, number of intervals not containing  $I$  has binomial distribution with parameters  $n = 100$  and  $p = 0.05$ . The probability that we will actually have  $\{3, \dots, 8\}$  such intervals is quite likely, it has probability 0.81. In all the figures we have between 3 and 8 such intervals. It all shows that the method works, thus the best method can be considered the one with shortest confidence interval – which is the cartesian stratified estimator with optimal allocation and  $m = 16$  strata (Fig. A1, right most) and stratified estimator with spherical stratified estimator with also optimal allocation and  $m = 16$  strata (Fig. A2, right most) being the second best. Summarizing, using stratified sampling results in the smallest uncertainty of estimation.

#### A.4.2 Example A1

Random variable  $X$  is a mixture of a uniform distribution  $\mathcal{U}(0.2, 0.4)$ , a normal  $\mathcal{N}(0.6, 0.0046)$  distribution and a beta distribution with parameters  $(\alpha, \beta) = (7, 1.1)$  with weights  $1/2, 1/4$  and  $1/4$  correspondingly. We train a flow model on sampled  $n = 1000$  points for 5000 epochs, the aim is to estimate  $\mathbb{P}(X \leq 0.95), \mathbb{P}(X \leq 0.99)$  and  $\mathbb{P}(X > 0.95)$ , as well as expectations of functions  $\rho_1(x) = \sin(e^x), \rho_2(x) = \log(1 + |x|), \rho_3(x) = 1/\log(1 + |x|)$ . We estimate it using trained flow model by sampling  $R = 2^{15}$  replications and using either CMC or stratified estimators (both, proportional and optimal) with  $m \in \{4, 8\}$  strata. In Table A4 we present results for more models and functions and we report also AC

Moreover, in Tables A5 and A6 we present results for Example A1, where the flow model was trained on 500 and 2000 points respectively. The conclusions are very similar to those for  $n = 1000$  (see Table A4), showing that even  $n = 500$  points are enough for flow model to learn the distribution correctly. This is also confirmed in Section 6, where we conducted a more detailed study on the influence of the sample size  $n$  on the quality of the trained flow model.

#### A.4.3 Example 2

In Table 2 we provided results for Example 2 in case  $d = 4$ . Here, in Table A7, we provide results for case  $d = 3$ . Conclusions are similar.

#### A.4.4 Example 3: Signed Distance Function (SDF)

In this experiment, the random vector  $\mathbf{X} = (X_1, X_2, X_3)^T$  has a density induced by a 3D mesh represented through a signed distance function (SDF) [16]. Figure A8 illustrates the mesh (left), a point cloud of 1000 mesh points (center), and a point cloud of 10000 points generated by the flow trained on 1000 points (right).

We consider the function  $j_t^+$  for  $t \in \{0.30, 0.50, 0.55\}$ . The reference value  $I$  is computed from a mesh of  $2^{22}$  points. The model is trained on 1000 examples and the estimation of  $I$  is performed using  $R \in \{2^{17}, 2^{18}\}$  points. For optimal allocation, we use  $R' = R$  pilot simulations.



Table A8: Example 3. Sample mesh (SDF).

Table A9 presents the results for cartesian stratification. Table A10 contains the results for spherical stratification. In both cases, stratified sampling provides lower empirical standard deviations compared to crude Monte Carlo, with optimal allocation yielding the smallest variability. Accuracy is highest for CMC and proportional allocation, while optimal allocation provides the most significant variance reduction.

#### A.4.5 Example 4 (real-world AmeriGEOSS data)

We considered estimating expectations of functions  $g_1, g_2, g_3$  and provided results (Table 3) of spherical stratification only. Here we additionally consider functions

$$g_4(x_1, x_2) = |\cos(e^{x_1 x_2})|, \quad g_5(x_1, x_2) = \log(x_1 + x_2), \quad g_6(x_1, x_2) = |\log |x_1 + x_2||^{-1}$$

and provide also results for cartesian stratification. Table A12 contains result for spherical stratification (thus, this is an extended version of Table 3), whereas Table A11 contains results for cartesian stratification. Moreover, in Fig. A3 we present 3000 (left) training data as well as 3000 points sampled from flow model trained on these points (right).

#### A.4.6 Example 5 (30D example)

In Table 4 we presented estimators  $\hat{Y}_{R,m=3}^{\mathcal{F},\text{prop},\text{Mrad}}$ ,  $\hat{Y}_{R,m=3}^{\mathcal{F},\text{opt},\text{Mrad}}$ , and  $\hat{Y}_{R,m=7}^{\mathcal{F},\text{prop},\text{Mrad}}$ . In Table A13 estimators  $\hat{Y}_{R,m=7}^{\mathcal{F},\text{opt},\text{Mrad}}$ ,  $\hat{Y}_{R,m=3 \times 3 \times 3}^{\mathcal{F},\text{prop},\text{MRand3}}$ , and  $\hat{Y}_{R,m=3 \times 3 \times 3}^{\mathcal{F},\text{prop},\text{MHigh3}}$  are provided.

We consider synthetic  $d = 30$  dimensional example with coordinates from different distributions. The distribution of  $\mathbf{X} = (X_1, \dots, X_{30})$  can be described as follows:

- $X_6, X_7, X_8, X_9, X_{21}, X_{22}, X_{23}, X_{24}$  are independent having standard normal  $N(0, \sigma^2)$  distributions with standard deviations 1, 1.2, 1.4, 1.6, 1, 1.2, 1.4 and 1.6.

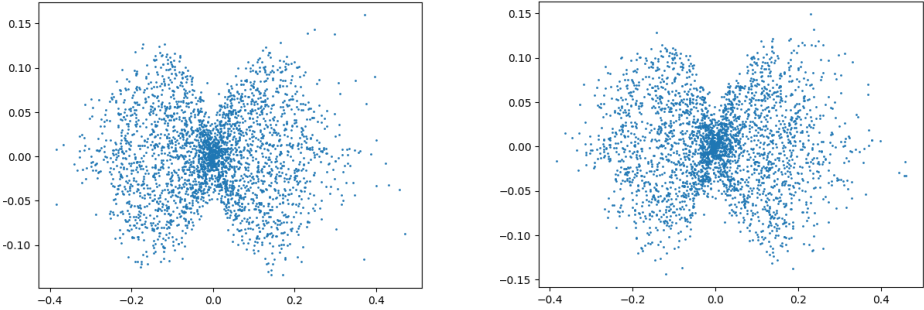


Fig. A3: Example 4: 3000 training points (left) and 3000 replications from trained flow model (right)

- $X_{10}, X_{11}, X_{12}, X_{13}, X_{25}, X_{26}, X_{27}, X_{28}$  are independent exponential  $\text{Exp}(\lambda)$  random variables with scales 0.4, 0.5, 0.6, 0.7, 0.4, 0.5, 0.6 and 0.7.
- $X_{14}, X_{15}, X_{29}, X_{30}$  are independent gamma random variables  $\Gamma(2, \beta)$  with parameters  $\beta$  being 1.6, 1.8, 1.6 and 1.8.
- $(X_1, \dots, X_5)$  and  $(X_{16}, \dots, X_{20})$  are two five-dimensional normal random vectors  $\mathcal{N}(\boldsymbol{\mu}_1, \boldsymbol{\Sigma}_1)$  and  $\mathcal{N}(\boldsymbol{\mu}_2, \boldsymbol{\Sigma}_2)$  respectively, where

$$\begin{aligned}
 \boldsymbol{\mu}_1 &= [-1, 1, 2, 1, 1]^T & \boldsymbol{\mu}_2 &= [1.0, -0.5, 0.0, 1.2, -0.8]^T \\
 \boldsymbol{\Sigma}_1 &= \begin{bmatrix} 55 & 8 & 17 & 19 & 23 \\ 8 & 8 & 8 & 9 & 11 \\ 17 & 8 & 13 & 15 & 20 \\ 19 & 9 & 15 & 23 & 24 \\ 23 & 11 & 20 & 24 & 32 \end{bmatrix} & \boldsymbol{\Sigma}_2 &= \begin{bmatrix} 1.0 & 0.8 & 0.6 & 0.4 & -0.3 \\ 0.8 & 2.0 & 1.0 & 0.7 & -0.5 \\ 0.6 & 1.0 & 1.5 & 0.9 & -0.4 \\ 0.4 & 0.7 & 0.9 & 1.2 & -0.2 \\ -0.3 & -0.5 & -0.4 & -0.2 & 1.0 \end{bmatrix}
 \end{aligned}$$

Fig. A4: Example 5: Pairplot 1000 points from  $d = 30$  dimensional distribution.

1000 points sampled from this 30D distribution are shown in Fig. A4. The figure contains a pairplot:  $i$ -th row and  $j$ -th column (for  $i \neq j$ ) is a scatter plot between  $X_i$  and  $X_j$ , whereas histograms are presented on the diagonal. We can see that most of the dimensions are independent, the dependent part is clearly visible (upper right corner and near the center of the plot). This synthetic example was created to reflect real-life scenarios, where we have data with multiple dimensions and that some of the variables are correlated. In our experiments we estimate  $I = P(X_1 \geq t, X_2 \geq t, \dots, X_{30} \geq t)$  (i.e.,  $\mathbb{E} j_t^+(\mathbf{X})$ ) for various values of  $t$ . For MHigh3 method we first perform  $R_0 = 2^{10}$  simulations per dimension to estimate  $\sigma^{\text{dim}}$ .

#### A.4.7 Example 6: 128-dimensional experiment

In this experiment, we consider the 128-dimensional latent space of the PointFlow model [22] trained on 4500 examples from the *chair* subset of the ShapeNet dataset [2]. The distribution in the latent space is modeled using a normalizing flow, and we used the publicly available trained model [14] to compute estimates of  $\mathbb{E} j_t^+(\mathbf{X})$  for  $t \in \{-0.45, -0.50, -0.55\}$ , where  $\mathbf{X} \in \mathbb{R}^{128}$ .

We applied three stratification approaches: (i) the **Mrad** method, stratifying the radius into  $m \in \{3, 5, 7, 9\}$  strata, (ii) the **MHigh3** method, and (iii) the **MRand3** method, both stratifying three selected coordinates into  $m_0 \in \{2, 4\}$  strata (yielding 8 or 64 strata in total).

Table A14 reports the results for  $n = 1000$  samples. Since the true value  $I$  is unknown, we present only the estimates **E** and the empirical standard deviations **SD**. In all but one case, a stratified method achieves the lowest **SD**. However, the differences between methods are relatively small.

Table A1: (Example 1) Numerical results for **cartesian** (method M1) stratification.

$f$	$I$	$\hat{Y}_{1000}^{obs}$			$R$	$\hat{Y}_R^{\mathcal{F},CMC}$			$\hat{Y}_{R,m=2 \times 2}^{\mathcal{F},prop,M1}$			$\hat{Y}_{R,m=2 \times 2}^{\mathcal{F},opt,M1}$		
		EST	SD*	ACC		EST	SD*	ACC	EST	SD*	ACC	EST	SD*	ACC
$j_{0.5}^+$	.3149	.3130	1.466	2.216	$2^{12}$	.3037	.7184	1.683	.3080	.6486	<b>1.795</b>	.3023	.6199	1.447
					$2^{15}$	.3070	.2548	<u>1.633</u>	.3065	.2295	1.576	.3055	.2219	1.537
$j_{1.2}^+$	.0324	.0270	.5126	.7757	$2^{12}$	.0314	.2722	1.247	.0323	.2655	1.360	.0316	.1674	<u>1.626</u>
					$2^{15}$	.0323	.0976	1.809	.0322	.0938	1.837	.0320	.0600	<u>2.144</u>
$j_{2.0}^+$	.0008	.0000	.0000	.0000	$2^{12}$	.0008	.0443	<u>.6127</u>	.0011	.0498	.4672	.0012	.0271	.5694
					$2^{15}$	.0010	.0178	.6684	.0011	.0179	.6904	.0010	.0102	<u>.7675</u>
$h_1$	.0333	.0277	.6144	.7722	$2^{12}$	.0314	.3102	1.408	.0337	.3025	1.363	.0328	.1878	1.447
					$2^{15}$	.0320	.1109	<u>1.507</u>	.0316	.1057	1.330	.0321	.0671	1.456
$h_2$	.0318	.0275	.3722	.8679	$2^{12}$	.0303	.1937	1.349	.0317	.1837	1.392	.0310	.1083	<u>1.593</u>
					$2^{15}$	.0307	.0692	1.504	.0306	.0638	1.488	.0309	.0383	<b>1.597</b>
$h_3$	.1230	.1014	1.718	.7548	$2^{12}$	.1165	1.072	1.100	.1255	1.236	1.091	.1203	.6756	<u>1.461</u>
					$2^{15}$	.1222	.6208	1.537	.1199	.4325	1.613	.1199	.2767	1.622

(a) Results for  $m = 2 \times 2$

$f$	$I$	$\hat{Y}_{1000}^{obs}$			$R$	$\hat{Y}_R^{\mathcal{F},CMC}$			$\hat{Y}_{R,m=4 \times 4}^{\mathcal{F},prop,M1}$			$\hat{Y}_{R,m=4 \times 4}^{\mathcal{F},opt,M1}$		
		EST	SD*	ACC		EST	SD*	ACC	EST	SD*	ACC	EST	SD*	ACC
$j_{0.5}^+$	.3149	.3130	1.466	2.216	$2^{12}$	.3037	.7184	1.683	.3080	.4303	<u>1.727</u>	.3054	.3123	1.526
					$2^{15}$	.3070	.2548	<u>1.633</u>	.3078	.1525	<b>1.651</b>	.3064	.1112	1.568
$j_{1.2}^+$	.0324	.0270	.5126	.7757	$2^{12}$	.0314	.2722	1.247	.0324	.2153	1.567	.0324	.0726	<b>1.819</b>
					$2^{15}$	.0323	.0976	1.809	.0324	.0760	1.846	.0322	.0259	<b>2.216</b>
$j_{2.0}^+$	.0008	.0000	.0000	.0000	$2^{12}$	.0008	.0443	<u>.6127</u>	.0009	.0460	.5850	.0009	.0128	<b>1.056</b>
					$2^{15}$	.0010	.0178	.6684	.0010	.0174	<b>.9000</b>	.0010	.0052	.6933
$h_1$	.0333	.0277	.6144	.7722	$2^{12}$	.0314	.3102	1.408	.0330	.2634	<u>1.538</u>	.0323	.1151	<b>1.548</b>
					$2^{15}$	.0320	.1109	<u>1.507</u>	.0323	.0945	<b>1.548</b>	.0321	.0415	1.463
$h_2$	.0318	.0275	.3722	.8679	$2^{12}$	.0303	.1937	1.349	.0310	.1430	<b>1.829</b>	.0307	.0599	1.501
					$2^{15}$	.0307	.0692	1.504	.0308	.0507	<u>1.549</u>	.0307	.0212	1.471
$h_3$	.1230	.1014	1.718	.7548	$2^{12}$	.1165	1.072	1.100	.1216	1.077	1.346	.1198	.3774	<b>1.627</b>
					$2^{15}$	.1222	.6208	1.537	.1211	.4327	<u>1.656</u>	.1205	.1789	<b>1.829</b>

(b) Results for  $m = 4 \times 4$

Table A2: (Example 1) Numerical results for **spherical** (method M2) stratification.

$f$	$I$	$\hat{Y}_{1000}^{obs}$			$R$	$\hat{Y}_R^{\mathcal{F},CMC}$			$\hat{Y}_{R,m=2 \times 2}^{\mathcal{F},prop,M2}$			$\hat{Y}_{R,m=2 \times 2}^{\mathcal{F},opt,M2}$		
		E	SD*	AC		E	SD*	AC	E	SD*	AC	E	SD*	AC
$j_{0.5}^+$	.3149	.3130	1.466	2.216	$2^{12}$	.3037	.7184	1.683	.3074	.6622	1.688	.3041	.6573	1.523
					$2^{15}$	.3070	.2548	1.633	.3076	.2341	<u>1.654</u>	.3069	.2330	1.619
$j_{1.2}^+$	.0324	.0270	.5126	.7757	$2^{12}$	.0314	.2722	1.247	.0327	.2715	1.227	.0330	.2210	1.301
					$2^{15}$	.0323	.0976	1.809	.0325	.0961	<u>1.889</u>	.0322	.0777	<b>1.992</b>
$j_{2.0}^+$	.0008	.0000	.0000	.0000	$2^{12}$	.0008	.0443	.6127	.0010	.0485	.3751	.0009	.0235	<u>.6191</u>
					$2^{15}$	.0010	.0178	.6684	.0010	.0173	<b>.9075</b>	.0011	.0103	.5958
$h_1$	.0333	.0277	.6144	.7722	$2^{12}$	.0314	.3102	<u>1.408</u>	.0305	.3046	1.279	.0306	.2568	1.091
					$2^{15}$	.0320	.1109	1.507	.0322	.1082	<b>1.580</b>	.0321	.0916	1.531
$h_2$	.0318	.0275	.3722	.8679	$2^{12}$	.0303	.1937	1.349	.0303	.1881	1.371	.0304	.1481	1.285
					$2^{15}$	.0307	.0692	<u>1.504</u>	.0309	.0676	<b>1.601</b>	.0305	.0533	1.437
$h_3$	.1230	.1014	1.718	.7548	$2^{12}$	.1165	1.072	1.100	.1162	1.099	1.183	.1211	.7953	1.346
					$2^{15}$	.1222	.6208	1.537	.1228	.5128	1.546	.1197	.3023	<u>1.679</u>

(a) Results for  $m = 2 \times 2$

$f$	$I$	$\hat{Y}_{1000}^{obs}$			$R$	$\hat{Y}_R^{\mathcal{F},CMC}$			$\hat{Y}_{R,m=4 \times 4}^{\mathcal{F},prop,M2}$			$\hat{Y}_{R,m=4 \times 4}^{\mathcal{F},opt,M2}$		
		E	SD*	AC		E	SD*	AC	E	SD*	AC	E	SD*	AC
$j_{0.5}^+$	.3149	.3130	1.466	2.216	$2^{12}$	.3037	.7184	1.683	.3080	.5567	<b>1.877</b>	.3074	.4569	<u>1.717</u>
					$2^{15}$	.3070	.2548	1.633	.3071	.1970	1.622	.3078	.1618	<b>1.662</b>
$j_{1.2}^+$	.0324	.0270	.5126	.7757	$2^{12}$	.0314	.2722	1.247	.0319	.2568	1.477	.0322	.1308	<b>1.547</b>
					$2^{15}$	.0323	.0976	1.809	.0321	.0912	1.745	.0322	.0467	1.880
$j_{2.0}^+$	.0008	.0000	.0000	.0000	$2^{12}$	.0008	.0443	.6127	.0012	.0522	.4157	.0010	.0123	<b>.9785</b>
					$2^{15}$	.0010	.0178	.6684	.0010	.0176	<u>.7266</u>	.0010	.0049	.6534
$h_1$	.0333	.0277	.6144	.7722	$2^{12}$	.0314	.3102	<u>1.408</u>	.0307	.2826	1.235	.0322	.1665	<b>1.524</b>
					$2^{15}$	.0320	.1109	1.507	.0316	.1006	1.355	.0321	.0585	<u>1.579</u>
$h_2$	.0318	.0275	.3722	.8679	$2^{12}$	.0303	.1937	1.349	.0301	.1758	<u>1.507</u>	.0311	.0993	<b>1.572</b>
					$2^{15}$	.0307	.0692	<u>1.504</u>	.0306	.0628	1.483	.0308	.0352	1.505
$h_3$	.1230	.1014	1.718	.7548	$2^{12}$	.1165	1.072	1.100	.1181	1.102	<u>1.418</u>	.1181	.4772	<b>1.620</b>
					$2^{15}$	.1222	.6208	1.537	.1184	.4030	1.403	.1204	.2099	<b>1.739</b>

(b) Results for  $m = 4 \times 4$

Table A4: (Example 2) Numerical results ( $R = 2^{15}$ ) for **cartesian** (method M1) stratification.

$f$	$I$	$\hat{Y}_{1000}^{obs}$			$\hat{Y}_R^{\mathcal{F},CMC}$			$\hat{Y}_{R,m=4}^{\mathcal{F},prop,M1}$			$\hat{Y}_{R,m=4}^{\mathcal{F},opt,M1}$		
		EST	STD*	ACC	EST	STD*	ACC	EST	STD*	ACC	EST	STD*	ACC
$j_{0.95}^-$	.9351	.8730	1.053	1.177	.8788	.1803	1.221	.8793	.1380	1.224	.8797	.0690	<b>1.227</b>
$j_{0.95}^+$	.0649	.1270	1.053	0.019	.1212	.1803	0.062	.1207	.1380	0.065	.1206	.0690	0.066
$j_{0.99}^-$	.9875	.9640	.5891	1.623	.9729	.0897	1.831	.9731	.0856	<b>1.837</b>	.9728	.0430	1.829
$\rho_1$	.8919	.8149	.6144	1.063	.8127	.1076	1.051	.8131	.0358	1.054	.8133	.0268	<u>1.055</u>
$\rho_2$	.4032	.4405	.5999	1.034	.4403	.1054	1.036	.4401	.0211	1.038	.4399	.0178	<u>1.040</u>
$\rho_3$	2.917	2.805	4.064	1.413	2.810	.7114	1.438	2.811	.1670	1.438	2.811	.1446	<u>1.438</u>

(a) Results for  $m = 4$ .

$f$	$I$	$\hat{Y}_{1000}^{obs}$			$\hat{Y}_R^{\mathcal{F},CMC}$			$\hat{Y}_{R,m=8}^{\mathcal{F},prop,M1}$			$\hat{Y}_{R,m=8}^{\mathcal{F},opt,M1}$		
		EST	STD*	ACC	EST	STD*	ACC	EST	STD*	ACC	EST	STD*	ACC
$j_{0.95}^-$	.9351	.8730	1.053	1.177	.8788	.1803	1.221	.8795	.0364	1.226	.8796	.0130	<u>1.226</u>
$j_{0.95}^+$	.0649	.1270	1.053	0.019	.1212	.1803	0.062	.1205	.0364	<b>0.067</b>	.1205	.0128	<u>0.066</u>
$j_{0.99}^-$	.9875	.9640	.5891	1.623	.9729	.0897	1.831	.9730	.0804	1.833	.9731	.0284	<u>1.836</u>
$\rho_1$	.8919	.8149	.6144	1.063	.8127	.1076	1.051	.8134	.0196	<b>1.055</b>	.8133	.0140	1.054
$\rho_2$	.4032	.4405	.5999	1.034	.4403	.1054	1.036	.4399	.0143	<b>1.040</b>	.4400	.0098	1.039
$\rho_3$	2.917	2.805	4.064	1.413	2.810	.7114	1.438	2.811	.1035	<b>1.441</b>	2.811	.0799	1.438

(b) Results for  $m = 8$ .

Table A5: (Example A1) Numerical results ( $R = 2^{15}$ ) for 500 training observations.

$f$	$I$	$\hat{Y}_{500}^{\text{obs}}$			$\hat{Y}_R^{\mathcal{F},\text{CMC}}$			$\hat{Y}_{R,m=4}^{\mathcal{F},\text{prop,M1}}$			$\hat{Y}_{R,m=4}^{\mathcal{F},\text{opt,M1}}$		
		E	SD*	AC	E	SD*	AC	E	SD*	AC	E	SD*	AC
$j_{0.95}^-$	.935	.746	1.94	0.69	.741	.241	.683	.741	.049	.682	.741	.024	<b>.684</b>
$j_{0.95}^+$	.065	.254	1.946	-0.46	.258	.241	-0.47	.258	.049	-0.47	.258	.024	<b>-0.47</b>
$j_{0.99}^-$	.987	.9280	1.156	1.22	.929	.141	1.23	.929	.124	<u>1.23</u>	.929	.062	1.22
$\rho_1$	.892	.657	.716	.580	.657	.088	<b>.580</b>	.657	.025	.580	.657	.023	<u>.580</u>
$\rho_2$	.4032	.6222	.2818	0.265	.6222	.0348	<b>.265</b>	.6222	.0164	.265	.6222	.0118	<u>.265</u>
$\rho_3$	2.917	1.62	.911	.354	1.62	.121	.354	1.62	.082	<b>.354</b>	1.62	.048	.354

(a) Results for  $m = 4$

$f$	$I$	$\hat{Y}_{500}^{\text{obs}}$			$\hat{Y}_R^{\mathcal{F},\text{CMC}}$			$\hat{Y}_{R,m=8}^{\mathcal{F},\text{prop,M1}}$			$\hat{Y}_{R,m=8}^{\mathcal{F},\text{opt,M1}}$		
		E	SD*	AC	E	SD*	AC	E	SD*	AC	E	SD*	AC
$j_{0.95}^-$	.935	.746	1.94	0.69	.741	.241	.683	.741	.048	.682	.741	.017	<u>.683</u>
$j_{0.95}^+$	.065	.254	1.946	-0.46	.258	.241	-0.47	.258	.049	-0.47	.258	.017	<u>-0.47</u>
$j_{0.99}^-$	.987	.9280	1.156	1.22	.929	.141	1.23	.929	.097	<b>1.23</b>	.929	.034	1.23
$\rho_1$	.892	.657	.716	.580	.657	.088	<b>.580</b>	.657	.012	.580	.657	.012	.580
$\rho_2$	.4032	.6222	.2818	0.265	.6222	.0348	<b>.265</b>	.6222	.0110	.265	.6222	.0065	.265
$\rho_3$	2.917	1.62	.911	.354	1.62	.121	.354	1.62	.074	<u>.354</u>	1.62	.046	.354

(b) Results for  $m = 8$

Table A6: (Example A1) Numerical results ( $R = 2^{15}$ ) for 2000 training observations.

$f$	$I$	$\hat{Y}_{500}^{\text{obs}}$			$\hat{Y}_R^{\mathcal{F},\text{CMC}}$			$\hat{Y}_{R,m=4}^{\mathcal{F},\text{prop,MI}}$			$\hat{Y}_{R,m=4}^{\mathcal{F},\text{opt,MI}}$		
		E	SD*	AC	E	SD*	AC	E	SD*	AC	E	SD*	AC
$j_{0.95}^-$	.9351	.9365	.5453	2.825	.9349	.1363	3.066	.9359	.1206	3.282	.9349	.0606	3.578
$j_{0.95}^+$	.0649	.0635	.5453	1.667	.0651	.1363	1.908	.0641	.1206	2.124	.0649	.0606	2.117
$j_{0.99}^-$	.9875	.9820	.2973	2.255	.9838	.0697	2.434	.9838	.0679	<b>2.439</b>	.9839	.0339	<u>2.436</u>
$\rho_1$	.8919	.8905	.3533	2.795	.8908	.0872	<u>2.897</u>	.8908	.0417	<b>2.912</b>	.8904	.0261	2.781
$\rho_2$	.4032	.4036	.3589	3.015	.4034	.0886	3.031	.4034	.0189	<b>3.198</b>	.4036	.0179	<u>3.034</u>
$\rho_3$	2.917	2.921	2.624	2.903	2.921	.6473	<b>3.118</b>	2.921	.1603	2.835	2.921	.1429	<u>2.950</u>

(a) Results for  $m = 4$

$f$	$I$	$\hat{Y}_{2000}^{\text{obs}}$			$\hat{Y}_R^{\mathcal{F},\text{CMC}}$			$\hat{Y}_{R,m=8}^{\mathcal{F},\text{prop,MI}}$			$\hat{Y}_{R,m=8}^{\mathcal{F},\text{opt,MI}}$		
		E	SD*	AC	E	SD*	AC	E	SD*	AC	E	SD*	AC
$j_{0.95}^-$	.9351	.9365	.5453	2.825	.9349	.1363	3.066	.9350	.0269	<u>3.591</u>	.9350	.0068	<b>3.995</b>
$j_{0.95}^+$	.0649	.0635	.5453	1.667	.0651	.1363	1.908	.0650	.0269	<u>2.433</u>	.0650	.0068	<b>2.807</b>
$j_{0.99}^-$	.9875	.9820	.2973	2.255	.9838	.0697	2.434	.9837	.0607	2.417	.9838	.0151	2.424
$\rho_1$	.8919	.8905	.3533	2.795	.8908	.0872	<u>2.897</u>	.8905	.0102	2.808	.8905	.0064	2.803
$\rho_2$	.4032	.4036	.3589	3.015	.4034	.0886	3.031	.4036	.0057	3.015	.4036	.0049	3.008
$\rho_3$	2.917	2.921	2.624	2.903	2.921	.6473	<b>3.118</b>	2.920	.0455	2.940	2.921	.0384	2.935

(b) Results for  $m = 8$

Table A7: (Example 2,  $d = 3$ ) Numerical results for **cartesian** (method M1) and **spherical** (method M2)

$f$	$I^*$	$\hat{Y}_{20k}^{\text{obs}}$			$R$	$\hat{Y}_R^{\mathcal{F},\text{CMC}}$			$\hat{Y}_{R,m=10 \times 10 \times 10}^{\mathcal{F},\text{prop},\text{M1}}$			$\hat{Y}_{R,m=10 \times 10 \times 10}^{\mathcal{F},\text{opt},\text{M1}}$		
		E*	SD*	AC		E*	SD*	AC	E*	SD*	AC	E*	SD*	AC
$h_1$	-0.03	.070	.066	-0.52	50k	-0.025	.044	-.121	-0.029	.042	-.130	-.017	.008	-.015
					100k	-0.039	.031	.174	-0.029	.030	.310	-.036	.006	<b>.475</b>
					500k	-0.019	.014	.560	-0.029	.013	.669	-.037	.003	<u>1.35</u>
$h_2$	.400	.376	.024	1.23	50k	.383	.015	<b>1.61</b>	.386	.010	<u>1.56</u>	.390	.002	1.53
					100k	.380	.011	1.37	.387	.007	<b>1.53</b>	.381	.001	1.35
					500k	.384	.005	1.41	.386	.003	1.47	.386	.001	1.45
$h_3$	1.36	1.27	.080	1.20	50k	1.30	.051	1.45	1.31	.037	<b>1.61</b>	1.36	.005	1.12
					100k	1.28	.036	1.35	1.30	.025	1.40	1.31	.004	1.34
					500k	1.30	.017	1.41	1.31	.012	1.44	1.31	.002	<b>1.55</b>

(a) Results for method M1

$f$	$I^*$	$\hat{Y}_{20k}^{\text{obs}}$			$R$	$\hat{Y}_R^{\mathcal{F},\text{CMC}}$			$\hat{Y}_{R,m=10 \times 10 \times 10}^{\mathcal{F},\text{prop},\text{M2}}$			$\hat{Y}_{R,m=10 \times 10 \times 10}^{\mathcal{F},\text{opt},\text{M2}}$		
		E*	SD*	AC		E*	SD*	AC	E*	SD*	AC	E*	SD*	AC
$h_1$	-0.03	.070	.066	-0.52	50k	-0.025	.044	-.121	-0.035	.040	<b>.247</b>	.004	.009	<u>.095</u>
					100k	-0.039	.031	.174	-0.027	.029	.182	-.021	.006	<u>.347</u>
					500k	-0.019	.014	.560	-.023	.013	.762	-.030	.003	<b>1.90</b>
$h_2$	.400	.376	.024	1.23	50k	.383	.015	<b>1.61</b>	.382	.011	1.39	.394	.002	1.25
					100k	.380	.011	1.37	.384	.008	<u>1.43</u>	.382	.001	1.27
					500k	.384	.005	1.41	.387	.003	<b>1.51</b>	.386	.001	<u>1.47</u>
$h_3$	1.36	1.27	.080	1.20	50k	1.30	.051	1.45	1.31	.043	<u>1.55</u>	1.34	.006	1.10
					100k	1.28	.036	1.35	1.31	.027	<b>1.52</b>	1.29	.004	<u>1.44</u>
					500k	1.30	.017	1.41	1.31	.012	<u>1.47</u>	1.31	.002	1.42

(b) Results for method M2.

Table A9: (Example 3) Numerical results for **cartesian** (M1) stratification.

$f$	$\hat{Y}_{1000}^{\text{obs}}$			$R$	$\hat{Y}_R^{\mathcal{F},\text{CMC}}$			$\hat{Y}_{R,m=8}^{\mathcal{F},\text{prop},\text{M1}}$			$\hat{Y}_{R,m=8}^{\mathcal{F},\text{opt},\text{M1}}$			$\hat{Y}_{R,m=64}^{\mathcal{F},\text{prop},\text{M1}}$			$\hat{Y}_{R,m=64}^{\mathcal{F},\text{opt},\text{M1}}$		
	E	SD*	AC		E	SD*	AC	E	SD*	AC	E	SD*	AC	E	SD*	AC	E	SD*	AC
$j_{0.3}^+$	.053	.708	1.1	$2^{17}$	.050	.060	1.8	.048	.055	1.9	.049	.033	2.1	.049	.051	<b>2.5</b>	.049	.025	<u>2.4</u>
				$2^{18}$	.049	.042	2.1	.050	.040	1.6	.049	.023	<b>3.2</b>	.050	.036	1.8	.049	.017	<u>2.4</u>
$j_{0.5}^+$	.004	.199	.89	$2^{17}$	.004	.019	<u>1.3</u>	.005	.019	.86	.005	.009	.99	.004	.018	<b>1.6</b>	.004	.005	1.2
				$2^{18}$	.004	.013	<b>1.4</b>	.005	.013	.99	.005	.007	1.1	.004	.013	<u>1.3</u>	.005	.004	1.1
$j_{0.55}^+$	.000	.000	.00	$2^{17}$	.001	.008	.23	.001	.008	.33	.001	.004	<b>.46</b>	.001	.009	.14	.001	.002	<u>.34</u>
				$2^{18}$	.001	.006	.30	.001	.006	.34	.001	.003	.38	.001	.005	<u>.44</u>	.001	.001	<b>.45</b>

Table A10: Example 3: numerical results for **spherical** (method M2) stratification.

$f$	$I$	$\hat{Y}_{1000}^{\text{obs}}$			$R$	$\hat{Y}_R^{\mathcal{F},\text{CMC}}$			$\hat{Y}_{R,m=8}^{\mathcal{F},\text{prop},\text{M2}}$			$\hat{Y}_{R,m=8}^{\mathcal{F},\text{opt},\text{M2}}$		
		E	SD*	AC		E	SD*	AC	E	SD*	AC	E	SD*	AC
$j_{0.3}^+$	.0494	.0532	.7085	1.146	$2^{17}$	.0501	.0603	<b>1.848</b>	.0550	.0610	.9479	.0563	.0515	.8565
					$2^{18}$	.0491	.0422	<b>2.126</b>	.0552	.0432	.9339	.0552	.0383	.9330
$j_{0.5}^+$	.0046	.0041	.1996	.8927	$2^{17}$	.0048	.0191	<u>1.277</u>	.0034	.0162	.6229	.0034	.0104	.5888
					$2^{18}$	.0047	.0134	<b>1.412</b>	.0032	.0109	.5148	.0032	.0069	.5090
$j_{0.55}^+$	.0006	.0000	.0000	.0000	$2^{17}$	.0009	.0083	.2921	.0004	.0061	.7934	.0005	.0038	.8513
					$2^{18}$	.0008	.0058	.3032	.0006	.00468	<b>1.595</b>	.0005	.0026	.7001

(a) Results for  $m = 8$ .

$f$	$I$	$\hat{Y}_{1000}^{\text{obs}}$			$R$	$\hat{Y}_R^{\mathcal{F},\text{CMC}}$			$\hat{Y}_{R,m=64}^{\mathcal{F},\text{prop},\text{M2}}$			$\hat{Y}_{R,m=64}^{\mathcal{F},\text{opt},\text{M2}}$		
		E	SD*	AC		E	SD*	AC	E	SD*	AC	E	SD*	AC
$j_{0.3}^+$	.0494	.0532	.7085	1.146	$2^{17}$	.0501	.0603	<b>1.848</b>	.0559	.0565	.8819	.0547	.0306	.9767
					$2^{18}$	.0491	.0422	<b>2.126</b>	.0553	.0398	.9268	.0549	.0216	.9562
$j_{0.5}^+$	.0046	.0041	.1996	.8927	$2^{17}$	.0048	.0191	<u>1.277</u>	.0005	.0046	<b>1.595</b>	.0004	.0026	1.226
					$2^{18}$	.0047	.0134	<b>1.412</b>	.0032	.0109	.5231	.0034	.0042	.5810
$j_{0.55}^+$	.0006	.0000	.0000	.0000	$2^{17}$	.0009	.0083	.2921	.0005	.0065	<b>1.239</b>	.0005	.0019	.9648
					$2^{18}$	.0008	.0058	.3032	.0005	.0043	.8491	.0005	.0013	.8269

(b) Results for  $m = 64$ .

Table A11: (Example 4) Numerical results for **cartesian** (method M1) stratification.

$F$	$\hat{Y}_{3000}^{\text{obs}}$		$R$	$\hat{Y}_R^{\mathcal{F},\text{CMC}}$		$\hat{Y}_{R,m=2 \times 2}^{\mathcal{F},\text{prop},\text{M1}}$		$\hat{Y}_{R,m=2 \times 2}^{\mathcal{F},\text{opt},\text{M1}}$		$\hat{Y}_{R,m=4 \times 4}^{\mathcal{F},\text{prop},\text{M1}}$		$\hat{Y}_{R,m=4 \times 4}^{\mathcal{F},\text{opt},\text{M1}}$	
	E	SD*		E	SD*	E	SD*	E	SD*	E	SD*	E	SD*
$g_1$	.1923	.7196	$2^{12}$	.1944	.6182	.1920	.3654	.1935	<u>.2368</u>	.1930	.2915	.1934	<b>.1389</b>
			$2^{15}$	.1943	.2186	.1935	.1287	.1935	<u>.0833</u>	.1933	.1037	.1932	<b>.0495</b>
$g_2$	.0009	.0877	$2^{12}$	.0010	.0749	.0007	.0457	.0012	.0459	.0009	<u>.0276</u>	.0009	<b>.0256</b>
			$2^{15}$	.0010	.0265	.0009	.0162	.0008	.0162	.0009	<u>.0098</u>	.0009	<b>.0091</b>
$g_4$	.0046	.0097	$2^{12}$	.0046	.0082	.0046	.0082	.0046	.0083	.0046	<u>.0053</u>	.0046	<b>.0045</b>
			$2^{15}$	.0046	.0029	.0046	.0029	.0046	.0029	.0046	<u>.0019</u>	.0046	<b>.0016</b>
$g_5$	.5402	.0109	$2^{12}$	.5402	.0092	.5402	.0070	.5402	.0070	.5402	<u>.0046</u>	.5402	<b>.0039</b>
			$2^{15}$	.5402	.0033	.5402	.0025	.5402	.0025	.5402	.0016	.5402	<b>.0014</b>
$g_6$	-2.847	2.839	$2^{12}$	-2.825	2.171	-2.837	1.988	-2.839	1.953	-2.829	<u>1.266</u>	-2.837	<b>1.141</b>
			$2^{15}$	-2.832	.7722	-2.835	.7075	-2.833	.6889	-2.832	<u>.4531</u>	-2.835	<b>.4017</b>
$g_7$	.4370	.3574	$2^{12}$	.4373	.3033	.4357	.2752	.4380	.2746	.4374	<u>.1690</u>	.4368	<b>.1611</b>
			$2^{15}$	.4371	.1078	.4366	.0976	.4369	.0970	.4371	<u>.0599</u>	.4365	<b>.0567</b>

Table A12: (Example 4) Numerical results for **spherical** (method M2) stratification. Full version of Table 3.

$F$	$\hat{Y}_{3000}^{obs}$		$R$	$\hat{Y}_R^{\mathcal{F},CMC}$		$\hat{Y}_{R,m=2 \times 2}^{\mathcal{F},prop,M2}$		$\hat{Y}_{R,m=2 \times 2}^{\mathcal{F},opt,M2}$		$\hat{Y}_{R,m=4 \times 4}^{\mathcal{F},prop,M2}$		$\hat{Y}_{R,m=4 \times 4}^{\mathcal{F},opt,M2}$	
	E	SD*		E	SD*	E	SD*	E	SD*	E	SD*	E	SD*
$g_1$	.1923	.7196	$2^{12}$	.1944	.6182	.1938	.5270	.1916	.3715	.1944	.2883	.1930	<b>.1758</b>
			$2^{15}$	.1943	.2186	.1926	.1862	.1929	.1315	.1937	<u>.1031</u>	.1931	<b>.0640</b>
$g_2$	.0009	.0877	$2^{12}$	.0010	.0749	.0008	.0372	.0007	.0349	.0007	<u>.0339</u>	.0010	<b>.0303</b>
			$2^{15}$	.0010	.0265	.0008	.0131	.0009	.0123	.0009	<u>.0120</u>	.0009	<b>.0107</b>
$g_4$	.0046	.0097	$2^{12}$	.0046	.0082	.0046	.0062	.0046	.0052	.0046	<u>.0051</u>	.0046	<b>.0039</b>
			$2^{15}$	.0046	.0029	.0046	.0022	.0046	<u>.0018</u>	.0046	.0018	.0046	<b>.0014</b>
$g_5$	.5402	.0109	$2^{12}$	.5402	.0092	.5402	.0092	.5402	.0075	.5402	.0046	.5402	<b>.0035</b>
			$2^{15}$	.5402	.0033	.5402	.0032	.5402	.0026	.5402	.0017	.5402	<b>.0012</b>
$g_6$	-2.847	2.839	$2^{12}$	-2.825	2.171	-2.836	1.914	-2.836	1.884	-2.833	<u>1.525</u>	-2.834	<b>1.326</b>
			$2^{15}$	-2.832	.7722	-2.834	.6742	-2.841	.6747	-2.833	<u>.5311</u>	-2.837	<b>.4685</b>
$g_7$	.4370	.3574	$2^{12}$	.4373	.3033	.4371	.2480	.4365	.2391	.4375	<u>.1733</u>	.4361	<b>.1592</b>
			$2^{15}$	.4371	.1078	.4366	.0872	.4367	.0840	.4370	<u>.0613</u>	.4365	<b>.0563</b>

Table A13: (Example 5) Results for Mrad, MHigh3 and MRand3 methods. Part 2.

$f$	$I^*$	$\hat{Y}_{n=500}^{obs}$			$R$	$\hat{Y}_R^{\mathcal{F},CMC}$			$\hat{Y}_{R,m=7}^{\mathcal{F},opt,Mrad}$			$\hat{Y}_{R,m=3 \times 3 \times 3}^{\mathcal{F},prop,MRand3}$			$\hat{Y}_{R,m=3 \times 3 \times 3}^{\mathcal{F},prop,MHigh3}$		
		E*	SD*	AC		E*	SD*	AC	E*	SD*	AC	E*	SD*	AC	E*	SD*	AC
$j_{-1.0}^+$	1.37	1.80	.595	.504	$2^{12}$	1.67	.200	.733	2.60	.141	.815	1.82	.208	.507	1.86	.210	.465
					$2^{13}$	1.67	.141	<b>.703</b>	1.55	.132	<b>.918</b>	1.74	.144	.605	1.68	.141	.697
$j_{-0.8}^+$	.560	.400	.282	.543	$2^{12}$	.735	.133	.635	.235	.043	.333	.699	.129	.642	.679	.127	.841
					$2^{13}$	.711	.092	.589	.444	.057	.918	.669	.089	<b>1.07</b>	.689	.091	.719
$j_{-0.6}^+$	.194	.000	.000	.000	$2^{12}$	.236	.075	<b>1.00</b>	.151	.047	.453	.191	.067	.821	.191	.067	<u>.972</u>
					$2^{13}$	.267	.056	.506	.070	.016	.264	.190	.048	<b>1.06</b>	.189	.047	<u>.924</u>

Table A14: (Example 7) numerical results for Mrad, MHigh3 and MRand3 methods.

$f$	$\hat{Y}_{4500}^{\text{obs}}$		$R$	$\hat{Y}_R^{\mathcal{F},\text{CMC}}$		$\hat{Y}_{R,m=3}^{\mathcal{F},\text{Mrad}}$		$\hat{Y}_{R,m=5}^{\mathcal{F},\text{Mrad}}$		$\hat{Y}_{R,m=7}^{\mathcal{F},\text{Mrad}}$		$\hat{Y}_{R,m=9}^{\mathcal{F},\text{Mrad}}$	
	EST	STD*		EST	STD*	EST	STD*	EST	STD*	EST	STD*	EST	STD*
$j_{-0.45}^+$	.029	.2491	$2^{17}$	.039	.0532	.038	<b>.0523</b>	.038	.0530	.038	.0530	.038	.0529
			$2^{18}$	.038	.0374	.038	.0373	.038	<u>.0373</u>	.038	.0373	.038	<b>.0373</b>
$j_{-0.50}^+$	.070	.3747	$2^{17}$	.080	<b>.0745</b>	.080	.0746	.080	.0747	.080	.0747	.080	<u>.0746</u>
			$2^{18}$	.080	.0530	.080	.0528	.080	.0528	.080	<u>.0528</u>	.080	.0529
$j_{-0.55}^+$	.128	.4921	$2^{17}$	.138	.0952	.137	<b>.0946</b>	.138	.0947	.137	.0946	.137	<u>.0946</u>
			$2^{18}$	.138	.0673	.138	.0670	.138	.0670	.137	<u>.0669</u>	.137	<b>.0669</b>

(a) Results for  $m \in \{3, 5, 7, 9\}$ .

$f$	$\hat{Y}_{4500}^{\text{obs}}$		$R$	$\hat{Y}_R^{\mathcal{F},\text{CMC}}$		$\hat{Y}_{R,m=2^3}^{\mathcal{F},\text{MHigh3}}$		$\hat{Y}_{R,m=2^3}^{\mathcal{F},\text{MRand3}}$		$\hat{Y}_{R,m=4^3}^{\mathcal{F},\text{MHigh3}}$		$\hat{Y}_{R,m=4^3}^{\mathcal{F},\text{MRand3}}$	
	EST	STD*		EST	STD*	EST	STD*	EST	STD*	EST	STD*	EST	STD*
$j_{-0.45}^+$	.029	.2491	$2^{17}$	.039	.0532	.039	<u>.0531</u>	.038	.0523	.039	.0531	.038	.0530
			$2^{18}$	.038	.0374	.038	.0374	.039	.0375	.038	.0373	.038	.0375
$j_{-0.50}^+$	.070	.3747	$2^{17}$	.080	<b>.0745</b>	.080	.0749	.080	.0749	.080	.0748	.080	.0749
			$2^{18}$	.080	.0530	.080	<b>.0528</b>	.080	.0529	.080	.0529	.080	.0529
$j_{-0.55}^+$	.128	.4921	$2^{17}$	.138	.0952	.138	.0951	.137	.0950	.137	.0950	.138	.0950
			$2^{18}$	.138	.0673	.137	.0672	.137	.0672	.137	.0671	.137	.0671

(b) Results for  $m \in \{2^3, 4^3\}$ .

## A.5 Training time

. Training (on a single GeForce RTX 2080) demanding Example 5 (30D) with CNF’s parameter `dims=128` (see A.3) takes  $\sim 3$ h (`dims=32` takes  $\sim 1$ h which gives slightly worse performance – not reported). Training Examples 1 and A1 takes  $\sim 1$ h. Note that in case of estimating many functions  $\mathbb{E}f_i(X)$ , the flow model must be trained only once.

## A.6 More details on choosing strata

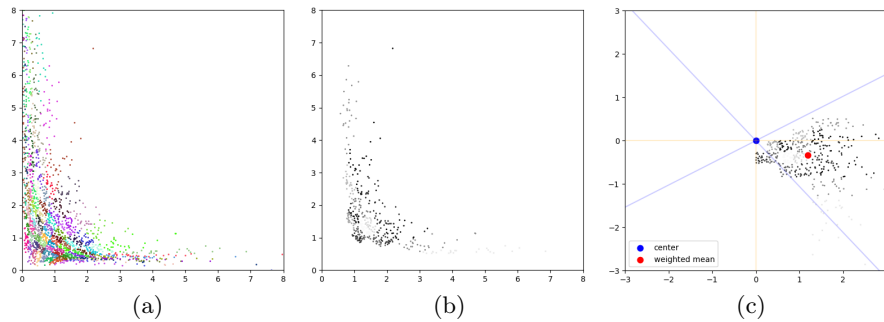


Fig. A5: Choosing strata in Example A1: (a)  $R = 2^{13}$  points from a base bivariate normal distribution sampled in 100 strata, transformed via flow model; (b) standard deviations (weights, the darker the larger) of a function  $h_1$  of points from given strata (all points in the same strata are assign the same weight); (c) points from (b) presented in base distribution, together with its weighted mean (red ball), rotation indicated by blue axis (rotated by  $29.33^\circ$ ).

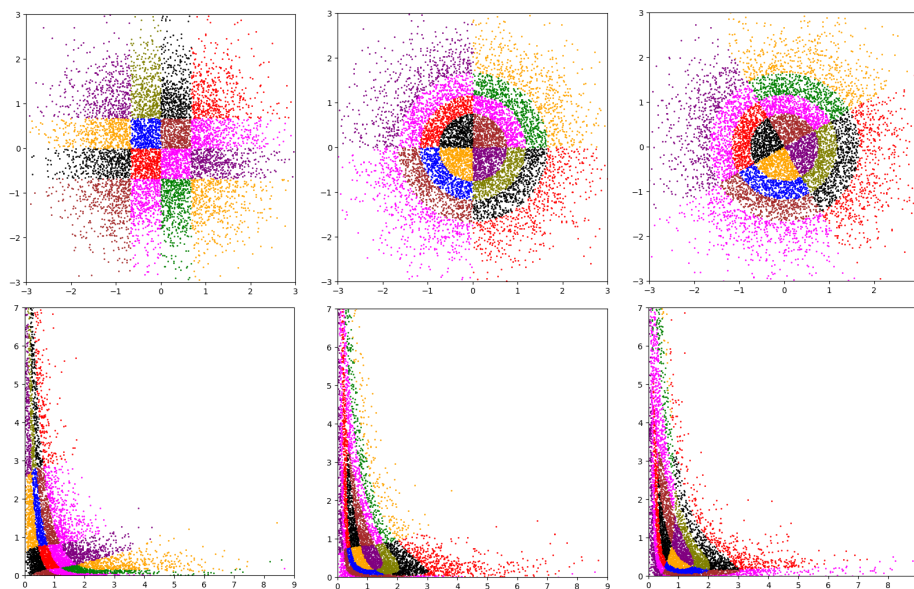


Fig. A6: Example A1:  $R = 2^{13}$  points and  $m = 16$  strata. Cartesian (1<sup>st</sup> column) and spherical (2<sup>nd</sup> and 3<sup>rd</sup> columns, in the latter strata are rotated by  $29.33^\circ$ ). First two columns were depicted in Fig. 3.

Note that even if we fix number of strata, we decide to have them equally probable, we may choose them in a variety of ways. E.g., in case of spherical method we may “rotate” strata (in all previous examples spherical strata started at angles 0, i.e., unrotated). As mentioned, a general design for choosing strata is left for a future work, here we shortly describe some reasonable approach for a 2-dimensional case. We will continue Example A1 with estimation of  $\mathbb{E} h_1(\mathbf{X})$ . The main idea is that the angle will depend on a function we want to estimate, and we will try to accommodate many points in a small number of strata. Simple method could be (for 2D) as follows. We start with some relatively large number of cartesian strata, say 100 (i.e., 10 in each dimension). For each stratum in a latent space we compute the standard deviation of estimated function. Then, each point is assigned a weight – the computed standard deviation. In Fig. A5: left – points sampled from 100 strata are presented; center – the darker the point the larger the standard deviation (most points invisible – std from corresponding strata either 0 or close to 0); right – the points in base (2D normal) distribution with their weights depicted. Afterwards we compute the weighted (with weights being the standard deviation) mean of the point (red ball in Fig. A5). The ball is at angle  $-15.67^\circ$ . Finally, we wish to have this ball in the middle of the strata – we rotate it  $-15.67^\circ + 45^\circ = 29.33^\circ$ . This way most of the points will be in this case in one stratum (disregarding radii). The rotated strata are depicted in the right-most column of Fig. A6.

Initial simulations show that it improves the accuracy: with  $R = 2^{15}$  the accuracy of a stratified estimator with optimal allocation yields accuracy 1.2271 in case of unrotated strata and 1.6056 in case of rotated strata.

We want to *emphasize* that this is just some heuristic approach, but it proves that choosing a strata based on a function we wish to estimate may results in better performance. A more in-depth study is left for a future work.